Annual Research Review of Laboratory of Chemistry and Materials Technology

2024

Volume 1

Editor: Vassilis Stathopoulos

National and Kapodistrian University of Athens

About this Review and LCMT

The Annual Research Review of 2024 provides a concise overview of the Laboratory of Chemistry and Materials Technology (LCMT) and its accomplishments under the direction of Professor Vassilis Stathopoulos during the calendar year 2023. This report aims to encapsulate the laboratory's advancements in chemistry and materials science, focusing on its commitment to sustainable technology innovation and provide access to the research data generated and reported within 2023.

LCMT, affiliated with the National and Kapodistrian University of Athens (NKUA), is a hub of interdisciplinary research at the forefront of materials science, and active part in the NKUA research institutes ecosystem. LCMT through Prof V. Stathopoulos is a member of Research Institute of Energy, Renewables and Transport and Research Institute of Biotechnology, Circular Bioeconomy and Sustainable Development - RIBIO3. Prof. Vassili Stathopoulos leads LCMT with a vision for sustainable solutions. His academic journey, including research stints in Germany and industrial experience, enriches LCMT's collaborative ethos. Professor Stathopoulos' leadership is marked by securing substantial funding, spearheading numerous research projects, and prolific publication in scientific journals. LCMT's research trajectory, under his guidance, emphasizes the development of materials with environmental and energy applications, positioning the laboratory as a key player in advancing sustainable technologies.

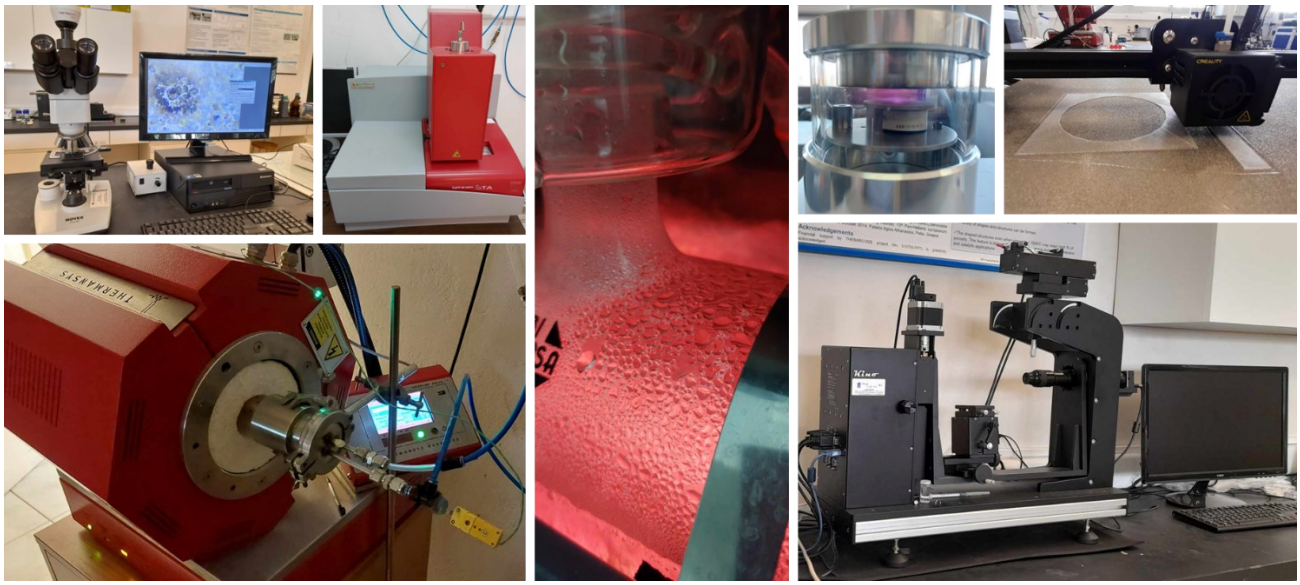

Table of Contents

Annual research aspects on chemistry and materials

Vassilis Stathopoulos[1, 2]

[1]Laboratory of Chemistry and Materials Technology, Core Department, National and Kapodistrian University of Athens, Psachna Campus, 34400, Evia, Greece

[2]Department of Agricultural Development, Agri-food and Management of Natural Resources, National and Kapodistrian University of Athens, Psachna Campus, 34400, Evia, Greece.

Abstract

This comprehensive review delves into the research activities and notable achievements of the Laboratory of Chemistry and Materials Technology (LCMT) throughout the year 2023. The publications, disseminated across esteemed scientific journals, encapsulate the innovative research endeavors undertaken at LCMT, ranging from fundamental discoveries to practical applications. In 2023, LCMT made a significant impact with nine scientific publications, and a international patent application and 39 contributions to conferences, where researchers presented their latest findings.

1. Introduction

The Laboratory of Chemistry and Materials Technology deals with research in the field of chemistry as well as materials technology. The symbiotic relationship between chemistry and materials technology is perhaps best exemplified by the interdisciplinary research endeavors pursued within the Laboratory of Chemistry and Materials Technology.

Chemistry, often referred to as the central science, serves as the cornerstone of our understanding of the natural world. It is the discipline that elucidates the composition, structure, properties, and transformations of matter, providing the fundamental framework upon which countless scientific endeavors rest. From elucidating the intricate mechanisms of biological processes to engineering novel materials with tailored properties, chemistry serves as the linchpin that connects disparate fields of study.

Materials technology, on the other hand, represents the practical manifestation of chemistry's theoretical underpinnings. It encompasses the design, synthesis, characterization, and application of materials with tailored properties to address a myriad of societal challenges. From lightweight and durable alloys revolutionizing aerospace engineering to nanostructured materials enabling next-generation electronics, materials technology empowers humanity to transcend the limitations of conventional materials and forge new frontiers of innovation.

Over the past decade, LCMT's prolific output in both publications and conference contributions exemplifies its enduring commitment to advancing the frontiers of knowledge in chemistry and materials technology. By embracing interdisciplinary approaches and

leveraging its collective expertise, LCMT continues to make significant contributions to scientific research, driving innovation and shaping the future of the field.

2. Scientific results and publications

Over the past decade, the Laboratory of Chemistry and Materials Technology (LCMT) has consistently demonstrated its prowess in scientific research, contributing a remarkable total of 79 publications that have significantly influenced the scientific community. Spanning a wide spectrum of research areas, these publications underscore the laboratory's multifaceted expertise and commitment to interdisciplinary collaboration. From catalysis to materials science, energy research to coatings (Fig. 1), LCMT's diverse portfolio reflects its dedication to addressing complex challenges through innovative solutions.

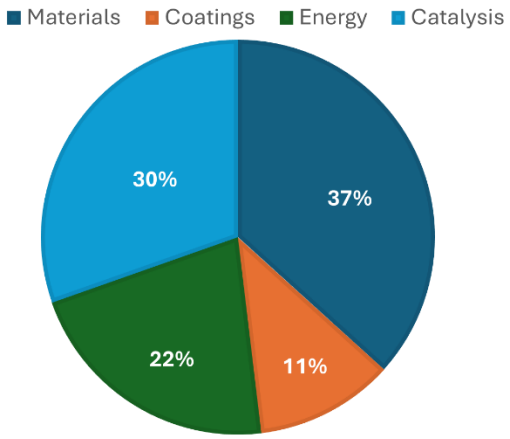

Figure 1. LCMT publication fields 2014-2024

Catalysis, representing 30% of LCMT's publications [1–19], stands as a cornerstone of the laboratory's research portfolio. Through meticulous experimentation and theoretical modeling, LCMT researchers have made significant strides in elucidating the intricate mechanisms governing catalytic processes. From the development of novel catalysts for organic transformations to the design of heterogeneous catalysts for sustainable chemical synthesis, LCMT's contributions to the field of catalysis have paved the way for greener, more efficient chemical processes with far-reaching implications for industry and society.

Materials science comprises the largest proportion of LCMT's publications [20–45], accounting for 37% of the laboratory's scientific output. Within this realm, LCMT researchers have harnessed the principles of chemistry and materials engineering to design and synthesize a diverse array of advanced materials with tailored properties. LCMT's contributions to materials science have transcended disciplinary boundaries, driving innovation across a myriad of fields and applications.

Energy-related research represents a significant focus of LCMT's endeavors, comprising 22% of the laboratory's publications [46–55]. Leveraging their expertise in chemistry and materials science, LCMT researchers have spearheaded efforts to develop sustainable energy solutions that mitigate the environmental impact of traditional energy sources. Whether it be the design of high-performance electrodes for energy storage devices

or the development of photocatalytic materials for solar energy utilization, LCMT's contributions to the energy sector have laid the groundwork for a more sustainable and resilient energy infrastructure.

Coatings, though representing a smaller proportion of LCMT's publications at 11% [56–62], nevertheless play a crucial role in multitude of technological applications. LCMT researchers have leveraged their expertise in surface chemistry and materials engineering to develop coatings with tailored functionalities, ranging from corrosion resistance and anti-fouling properties to stimuli-responsive behavior. These coatings find application in diverse fields such as aerospace, automotive, and biomedical engineering, where they enhance the performance, durability, and functionality of critical components and devices.

Collectively, LCMT's scientific publications over the past decade underscore the laboratory's unwavering commitment to advancing the frontiers of knowledge in chemistry and materials technology. Through a combination of fundamental research, applied science, and interdisciplinary collaboration, LCMT researchers continue to push the boundaries of scientific inquiry, driving innovation and fostering positive societal impact in the process. The publications from 2023, as summarized in Table 1, are thoroughly examined next, for their insights and implications.

Table 1. LCMT publications 2023

No	Publication title	page	Reference
2.1	Metal-Organic-Framework-based nanofiltration membranes for selective multi-cationic recovery from seawater and brines	6	[63]
2.2	Fabrication of highly active and stable Ni/CeO2-nanorods wash-coated on ceramic NZP structured catalysts for scaled-up CO2 methanation	6	[1]
2.3	Multi-Layer Ceramic Capacitors in Lighting Equipment: Presence and Characterisation of Rare Earth Elements and Precious Metals	7	[20]
2.4	Performance Comparison of Different Cathode Strategies on Air-Cathode Microbial Fuel Cells: Coal Fly Ash as a Cathode Catalyst	7	[2]
2.5	Construction, Evaluation, and Performance of a Water Condensation Test Unit	7	[64]
2.6	Micromachining on Stainless Steel 304 for Improved Water Condensation Properties	14	[56]
2.7	Bioenergy Production from Tannery Waste via a Single-Chamber Microbial Fuel Cell with Fly Ash Cathodic Electrodes	19	[65]
2.8	Development and Evaluation of Corrosion Resistance and Hydrophobic Properties of Thermal Sprayed Coatings over Carbon Steel	24	[57]
2.9	Fabrication and Study of 3D Printed ABS-Carbon Composite Anodes for Single Chamber Microbial Fuel Cells	30	[66]

Description of published works

2.1. Metal-Organic-Framework-based nanofiltration membranes for selective multi-cationic recovery from seawater and brines, https://doi.org/10.1016/j.memsci.2023.121941

Nanofiltration (NF) has emerged as a crucial component in Zero Liquid Discharge (ZLD)/Minimal Liquid Discharge (MLD) systems, playing a pivotal role in improving the efficiency of downstream processes for reclaiming valuable minerals from seawater and brines. However, a persistent challenge lies in ensuring that the purity of the extracted minerals meets market specifications, rendering ZLD/MLD economically unviable at present. To address this challenge, this study focuses on the development of a novel positively charged NF membrane aimed at enhancing selectivity for magnesium and calcium. The membrane design comprises two key components: an ultrafiltration substrate and an active layer incorporating NH2-MIL-101(Al) and ZnO nanoparticles within a chitosan matrix. The investigation explores the impact of varying loadings of NH2-MIL-101(Al) and ZnO on membrane structure, selectivity, and water permeability. Initial filtration experiments using single-salt solutions at 1000 ppm (NaCl, Na_2SO4, $MgCl_2$, CaCl2) reveal that the membrane containing 35%wt of ZnO exhibits the highest rejections of MgCl2 (90.10%) and $CaCl_2$ (86.49%). Furthermore, the selectivity towards $MgCl_2$ and $CaCl_2$ surpasses that of commercial membranes such as NF90 and NF270, as well as positively charged membranes introduced in recent literature. Subsequent tests with synthetic seawater and brine, conducted at a trans-membrane pressure of 30 bar, underscore the compelling competitive edge of the newly synthesized membrane in terms of magnesium and calcium selectivity when compared to NF90 and NF270, particularly in the context of seawater and brine valorization efforts. [63]

2.2. Fabrication of highly active and stable Ni/CeO2-nanorods wash-coated on ceramic NZP structured catalysts for scaled-up CO2 methanation, https://doi.org/10.1016/j.jcou.2023.102425.

The synthesis of synthetic natural gas through CO_2 methanation using green H2 produced via water electrolysis presents a promising solution for managing excess power from variable renewables and reducing CO_2 emissions. Nickel-based catalysts, particularly supported on ceria nanorods, have shown exceptional low-temperature CO_2 methanation activity due to enhanced metal-support synergy. This study focuses on scaling up the CO_2 methanation process by fabricating highly porous NZP-type ceramic substrates and wash-coating them with Ni/CeO_2-nanorods catalyst. Scaled-up experiments, conducted with a mass and volume of catalysts 80:1 and 65:1 times larger than lab-scale experiments, respectively, demonstrated the remarkable performance and stability of the structured catalyst. A methane formation rate of 277 NL g_{Ni}^{-1} h^{-1} was achieved, surpassing values reported in similar studies. Additionally, it was observed that increased space velocity resulted in higher temperature gradients in the catalytic bed, favoring CO generation. Importantly, the catalyst's morphological and structural characteristics remained unchanged even after multiple on/off

reaction cycles and stability tests, indicating potential for scaling up the process using real feed streams at higher technology readiness levels. [1]

2.3. Multi-Layer Ceramic Capacitors in Lighting Equipment: Presence and Characterisation of Rare Earth Elements and Precious Metals, https://doi.org/10.3390/recycling8060097.

The drive to diminish energy usage in buildings has led to a notable shift in lighting technology, particularly with the advent of light-emitting diode (LED) lamps circa 2010. These LEDs, boasting extended lifespans, have become pivotal in the quest to exclusively utilize LED lamps by 2025, consequently reshaping the landscape of Category 3 waste electrical–electronic equipment (WEEE) and fostering expectations for streamlined, high-concentration recycling pathways. This research endeavors to examine multi-layer ceramic capacitors (MLCCs) extracted from WEEE within the lighting sector, focusing on the identification of rare earth elements (REEs) and precious metals (PMs) they contain. To achieve this, the MLCCs underwent a digestion process employing HNO3 and aqua regia on a heated plate, followed by characterization utilizing inductively coupled plasma optical emission spectroscopy (ICP-OES) and scanning electron microscopy with energy-dispersive X-ray spectroscopy (SEM-EDX). Analysis revealed that the MLCCs harbor a weight percentage of 0.84% REEs and 0.60% PMs, constituting an economically significant reservoir, primarily driven by PMs accounting for 98.67%, with palladium (Pd) dominating at 78.37%. Further breakdown showcased the prevalence of key elements: neodymium (Nd) at 0.366%, yttrium (Y) at 0.220%, dysprosium (Dy) at 0.131%, silver (Ag) at 0.467%, and Pd at 0.105%. These findings underscore the necessity for targeted extraction methods and segregated recycling procedures specifically tailored for MLCCs sourced from WEEE in lighting applications. [20]

2.4. Performance Comparison of Different Cathode Strategies on Air-Cathode Microbial Fuel Cells: Coal Fly Ash as a Cathode Catalyst, https://doi.org/10.3390/w15050862.

The study explored the impact of various cathode configurations, including mullite/MnO_2, Plexiglas/Gore-Tex/MnO_2, mullite/coal fly ash, mullite/biochar, and mullite/activated carbon, on the performance of air-cathode microbial fuel cells (MFCs). Among these configurations, the combination of MnO_2 catalyst applied on Gore-Tex cloth exhibited the highest maximum power output (7.7 mW/m^3). However, the highest coulombic efficiencies (CEs) were attained with MnO_2 (CE 23.5 ± 2.7%) and coal fly ash (CE 20 ± 3.3%) applied on ceramic substrates. These findings underscore the potential of utilizing coal fly ash and biochar as catalysts in MFC technology, offering both sustainability and cost-effectiveness.[2]

2.5. Construction, Evaluation, and Performance of a Water Condensation Test Unit, https://doi.org/10.4028/p-am2ENG

The study of water condensation phenomena is important in order to evaluate the performance of materials and coatings employed in the fabrication of waste heat recovery units including heat exchangers, heat pipes, condensing economizers and related functional surfaces. Fast evaluation of lab-scale samples is important during research and development of coatings for wetting phenomena under controlled, reproducible, and stable

humidity and temperature conditions of both sample and environment. To study these effects, we report on the construction of a lab-scale condensation chamber, along with its evaluation and benchmarking with superhydrophobic coatings on stainless steel using perfluorooctyl silane (PFOTS). A working unit has been successfully fabricated and applied in a highly responsive device capable of recording the condensation performance of flat specimens under controlled conditions. Sample temperature was maintained with 0.10 °C deviation. The humidity response time of the chamber is 17.2 s per degree of RH% while the maximum relative humidity variation is +/- 3.2%RH. The unit successfully delivered valuable data over hydrophillic, hydrophobic and superhydrophobic surfaces. Data useful for studying open research issues such the relationship of contact angle and condensation phenomena.[64]
The comprehensive edition of this publication can be found in Figure 2.

Advances in Science and Technology
ISSN: 1662-0356, Vol. 133, pp 35-43
doi:10.4028/p-am2ENG

Submitted: 2022-10-12
Revised: 2023-03-06
Accepted: 2023-04-19
Online: 2023-10-19

Construction, Evaluation, and Performance of a Water Condensation Test Unit

Paraskevi Nanou[1,2,a], John Konstantaras[1,b], Athanasios Zarkadoulas[1,2,c], Pavlos K. Pandis[1,d], Nikolaos Vourdas[1,e], and Vassilis Stathopoulos[1,f*]

[1]Laboratory of Chemistry and Materials Technology, Department of Agricultural Development, Agrofood and Management of Natural Resources, National and Kapodistrian University of Athens, Psachna Campus, 34400, Evia, Greece.

[2]University of Thessaly, Gaiopolis Campus – Ring Road of Larissa-Trikala, GR41500 Larissa Greece.

[a]nanoupar@uoa.gr, [b]yiannis.konstantaras@gmail.com, [c]azarkadoulas@uoa.gr, [d]ppandis@uoa.gr, [e]n.vourdas@inn.demokritos.gr, [f]vasta@uoa.gr

Keywords: condensation, drop-wise condensation, film-wise condensation, waste heat recovery, condensation chamber, hydrophobic

Abstract. The study of water condensation phenomena is important in order to evaluate the performance of materials and coatings employed in the fabrication of waste heat recovery units including heat exchangers, heat pipes, condensing economizers and related functional surfaces. Fast evaluation of lab-scale samples is important during research and development of coatings for wetting phenomena under controlled, reproducible, and stable humidity and temperature conditions of both sample and environment. To study these effects, we report on the construction of a lab-scale condensation chamber, along with its evaluation and benchmarking with superhydrophobic coatings on stainless steel using perfluorooctyl silane (PFOTS). A working unit has been successfully fabricated and applied in a highly responsive device capable of recording the condensation performance of flat specimens under controlled conditions. Sample temperature was maintained with 0.10 ºC deviation. The humidity response time of the chamber is 17.2 s per degree of RH% while the maximum relative humidity variation is +/- 3.2%RH. The unit successfully delivered valuable data over hydrophillic, hydrophobic and superhydrophobic surfaces. Data useful for studying open research issues such the relationship of contact angle and condensation phenomena.

1. Introduction

Today a transition towards a cleaner, less polluting energy system is of paramount importance. The European Commission has already presented its Clean Energy for all Europeans package with a set of actions to Accelerate Clean Energy Innovation, targeting energy efficiency. In this direction waste heat recovery is an approach for improving energy efficiency in processes. For example, by applying condensing heat exchangers, in which the latent heat of the flue gases is exploited, can increase energy efficiency in conventional systems. The facilities that exploit the latent heat of the flue gases are usually referred to as condensing economizers, condensing heat exchangers etc [1]. In order to widen the application potential of technologies and devices exploiting the latent heat of the flue gases three issues related to the engineered heat exchange surface should be met: i) corrosion protection [2-4], ii) promotion of dropwise condensation (DwC) over filmwise condensation (FwC) [5] and iii) ease of self-removal of the condensates which yield increased heat transfer coefficient (HTC) [6].

Corrosion issue of condensing surfaces can be addressed either by the incorporation of expensive metals as engineering materials exhibiting low corrosion rates or by applying functional coatings to protect a much more cost-efficient base material. Ceramic or thinner coatings are able to provide protection in metal substrates at extreme conditions or both protect and modify the wetting properties at the same time of the condensing interface [7-12].

Due to the nature of gas to liquid phase change, the process, that involves mass and heat transfer at the interface of the vapor, surface, and liquid can be limited by the surface properties. Therefore, a vast research effort is attracted towards tailoring surfaces physical and chemical properties so that phase change efficiency can be enhanced without the need of any external active means. Two forms of condensation are known: filmwise condensation (FWC) responsible for the formation of a condensate layer on the heat transfer surface and dropwise condensation (DWC) delivering condensate through a population of droplets that are removed by gravity or shear after reaching a suitable size. It is thus well established that development of coatings and materials that exhibit FwC, and eventually novel surfaces that allow DwC or even self-jumping water condensation can yield higher efficiencies in latent heat and steam recovery in industrial processes [1,13,14]. DwC can deliver heat transfer coefficients increased by a factor of 2 compared to FwC [15]. This results not only in the development of more economic procedures due to recovery of heat and water, but also to greener, safer, and more sustainable practices in chemical and manufacturing procedures [13-17]. The above approach is applied in iWAYS project where a set of technologies capable of recovering water and energy from challenging exhaust streams is being developed, for productive use in three different energy and resources intensive industrial sectors: ceramic tile manufacturing, aluminium fluoride production and steel tubes manufacturing. Thus, additional materials can be recovered from flue gas via condensation such as valuable acids or particulates, improving the production's raw material efficiency and reducing detrimental emissions to the environment [16].

Study of condensation phenomena using standard practices, for example ASTM D2247-15(2020) and ASTM D4585/D4585M-18, is limited to large scale experiments that do not allow tests usually employed in research laboratories or small R&D facilities.

Based on our experience studying wetting phenomena and water condensation [13, 17-19], there is a need for quick evaluation of small specimens-candidates for the desired applications, for example equipment assembled for studying surfaces of condensation phenomena reported earlier in the literature [20, 21]. However, when exploring various parameters such as coating composition and material stress under various conditions, careful manipulation of different variables is needed to explore the versatility and limits of the designed material or coating. Controlled relative humidity is also of high importance, since the variable content of flue gases exhibits different dew points. Such crucial aspects are merely not met by the units reported.

Herein we report the design, construction, manufacture, and working evaluation of a unit to examine condensation phenomena over flat specimens in a controlled environment in terms of relative humidity and temperature. The unit was fabricated to be easily controlled and provide quick results even if condensation conditions need to change, or in stable conditions, with a fast response regarding relative humidity and low deviation in temperature values. Unit delivered valuable data over hydrophillic, hydrophobic and superhydrophobic surfaces.

2. Construction of the Test Unit

A unit was constructed for increased accuracy and control over the conditions of interest. More specifically, the chamber apparatus consists of three parts: Main chamber, relative humidity (RH) and temperature controls, and sample temperature control, as described in the following sections:

3.1 Main Chamber. Plexiglas (Poly methyl methacrylate) was chosen as the shell-outer case material for the main test chamber. Plexiglass is lightweight, does not shatter like glass, and at the same time it can be easily machined, drilled, cut, and glued according to desire. Also, it exhibits chemical resistance against dilute acidic and basic media, a lower thermal conductivity than glass, and low water absorption [22]. Moreover, condensation phenomena can be visually inspected and easily monitored and recorded using a video camera, due to its high optical light transmission and UV-resistance which increases its lifetime. The main chamber (Fig. 1) is designed with a cubical shape with external dimensions: 17cm x 21cm x 17cm (LxWxH). One face of the chamber is cut to accommodate the test sample while the top face is removable for cleaning and maintenance purposes. The humid air mixture in introduced to the chamber through a hole at the bottom of the chamber and

Figure 2. Comprehensive edition of "Construction, Evaluation, and Performance of a Water Condensation Test Unit

exits at the top. Two relative humidity and temperature (RHT) sensors are placed in the chamber to monitor temperature and relative humidity and a strip heating element at the bottom regulates the chamber temperature. The strip heater is controlled with a variable transformer (Variac).

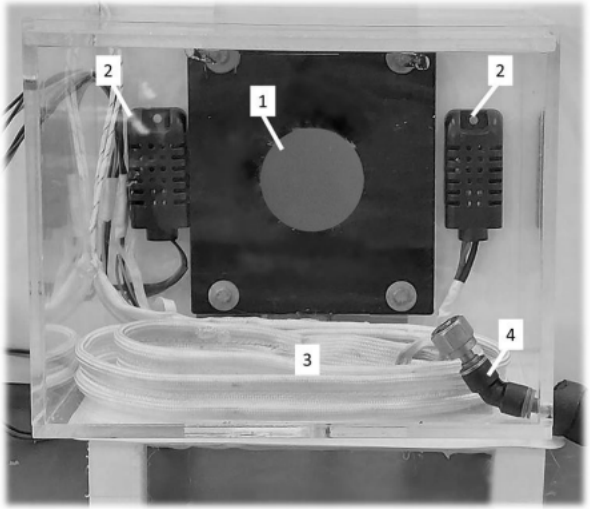

Figure 1. Photo of the test chamber. 1: Test Sample, 2: Temperature & Relative Humidity Sensors, 3: Heating Resistor, 4: Processed Air Inlet to the Chamber

3.2 Relative Humidity (RH) and Temperature Control. The control of relative humidity and temperature inside the test chamber is of great importance for the operation of the device as a testing chamber. To achieve stable and controllable conditions inside the chamber the inlet air-water vapor is processed in steps as shown in Fig. 2. The environmental air is delivered with the use of an oil-free air compressor. A pressure regulator is used to control the air pressure in the system. After the pressure regulator, the air is dried through a silica gel desiccator. The dry air is then pre-heated, by passing through a helical tube wrapped with an electric strip heater. The pre-heater is controlled with a Variac to maintain air temperature at T1 (measured right after the heater) equal to the desired saturation temperature (as shown in Fig. 3). The heated air then enters the steam generator to absorb humidity. The temperature of the water in the steam generator is measured and controlled to be the same as T1. The saturated air stream after the steam generator is further heated to the desired chamber temperature (T2) with the use of another heater which is of the same design as the pre-heater. A portion of the processed air is vented at the air splitter outlet to enable the control of the inlet air volume to the test chamber which is measured with the use of a flow meter/regulator. Finally, the temperature of the test chamber is controlled with the use of a strip heater installed at the bottom of the chamber. The temperature and humidity inside the chamber are measured with two RHT (Relative Humidity and Temperature) sensors and the measurements are logged in a personal computer.

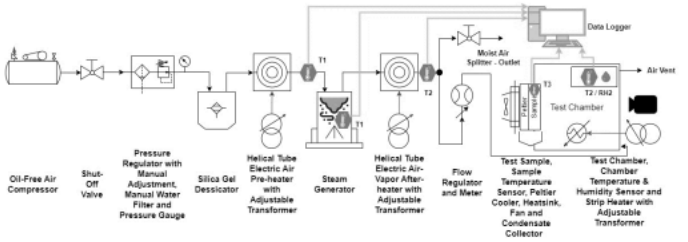

Figure 2. Diagram of the temperature and humidity control unit.

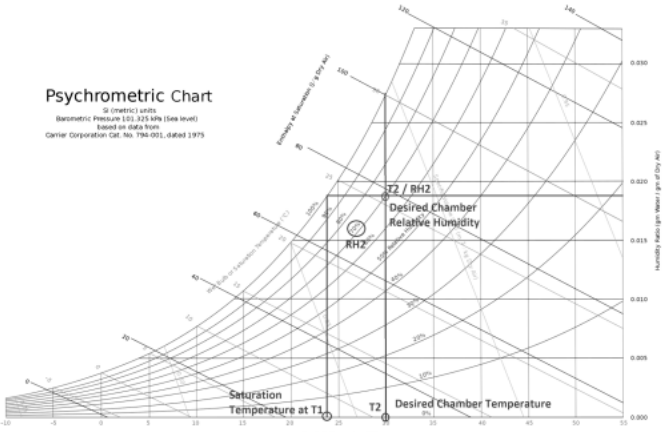

Figure 3. Air processing steps on the psychrometric chart.

3.3 Sample temperature control. The temperature of the sample is controlled with the aid of a Peltier module in contact with the flat specimen. The Peltier module is placed outside the test chamber with the cold face of the module in contact with the sample and the hot face in contact with a heatsink cooled by a fan motor. By regulating the Peltier current/voltage supply the temperature of the sample is controlled. The sample temperature is measured with a sensor installed at the back of the sample and logged in a personal computer.

Figure 3. (continued)

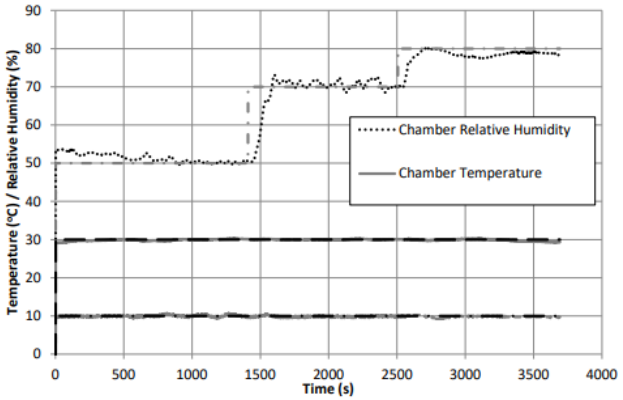

Figure 4. Chamber performance test results.

3. Benchmarking and Water Condensation

4.1 Test chamber performance. For the performance evaluation of the chamber a response test is performed. The desired temperature inside the chamber is set at 30 °C, the desired sample temperature is 10 °C, and the desired humidity is varied in steps with thresholds at 50%, 70% and 80% relative humidity. Each threshold has a set duration of about 20 min. The results are presented in Fig. 4. Based on the results, the control characteristics of the chamber are evaluated in terms of response time, stability and accuracy for each of the controlled conditions. The sample temperature (as controlled by the Peltier module) exhibits excellent stability (+/- 0.75 °C) over the entire test time while accuracy is also very high with average sample temperature of 9.90 °C which responds to 0.10 °C deviation from the set point temperature. The chamber temperature when set at 30.00 °C shows a variation of +0.30 °C/-0.90 °C which is acceptable for the intended application while the average value is calculated to be 29.91 °C. The relative humidity in the chamber is the most important characteristic of the device as it greatly affects the water collection rate of the samples. The response time of the chamber in the changes of the humidity threshold is calculated to be 17.2 s/RH% (meaning that 17.2 seconds are required for a change of 1% in the value of relative humidity). Relative humidity variation is calculated to be +/- 3.2%RH, which represents the worst case among the three operating conditions tested and accuracy is 1.4%RH considering the lowest accuracy of the three operating conditions. The performance results are summarized in Table 1:

Table 1. Performance results

Control Variable	Response Time	Variation	Deviation
Sample Temperature	-	+/-0.75 °C	0.10
Chamber Temperature	-	+0.30°C/-0.90 °C	0.09 °C
Chamber Humidity	17.2s/RH%	+/-3.2%RH	1.4%RH

4.2 Water condensation. As a proof of concept, a commercial metal specimen was evaluated, before functionalization and after two different surface modification processes (Fig. 5). The specimens were coated with a superhydrophobic silane (PFOTS) as previously reported [9,24-26]. The different surface functionalization delivers specimens of variable contact angles, ranging from hydrophilic to superhydrophobic, as Fig. 5 shows. Pristine specimens' performance can be clearly monitored and recorded as shown in Fig. 5a and 5b after exposure to 80% relative humidity at 30 °C for 5 and 30 min respectively. This sample exhibits the formation of deformed, elongated droplets indicative of a filmwise water condensation mechanism, which is anticipated by its relatively hydrophilic nature as revealed by the contact angle measurement of 80° [27]. The second sample is superhydrophobic, exhibiting a contact angle of 166°. This sample, after 5 and 30 min of exposure to the same conditions as above, clearly shows a dropwise condensation effect (Fig. 5c and 5d). Condensation occurs by forming fine, clearly defined droplets that readily slide off, much easier than for the case of the non-functionalised sample in the same timeframe. However, the third functionalised specimen, with contact angle equal to 103°, exhibits different performance under the exact same condensation conditions applied in the testing chamber. Fig. 5f shows that the condensation mode is strictly film-wise. A remarkably different behavior than the one recorded by the pristine hydrophilic surface. Such diverse results among a hydrophilic and a hydrophobic surface indicates the importance of observing the wetting behavior under condensing conditions as applied in the present test unit. These results come into agreement with what reported over the recent years that a higher contact angle is not a necessary condition for not showing FWC or for exhibiting DWC [28].

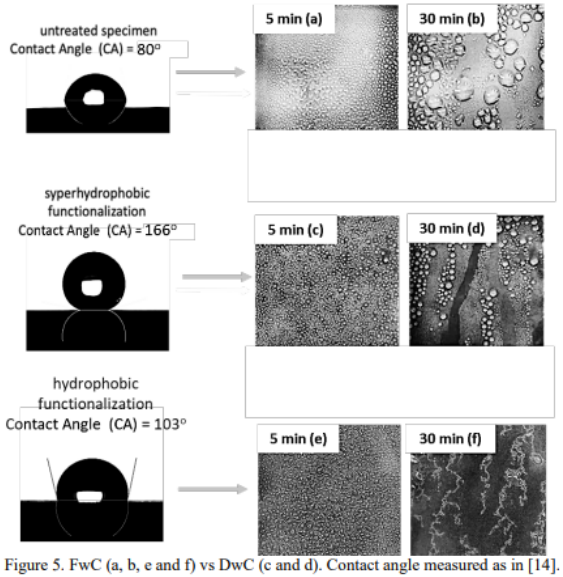

Figure 5. FwC (a, b, e and f) vs DwC (c and d). Contact angle measured as in [14].

Figure 4. (continued)

4. Conclusions

Nowadays the need for improved overall efficiency in a wide range of energy and environmental applications is growing. Such applications that include water harvesting and desalination, air-cooling, power generation as well as thermal management and waste heat recovery involve gas to liquid phase transitions through condensation. This results in novel coatings, materials and engineered surfaces for the construction of devices that can utilise efficiently the latent heat released during condensation with direct practical applications in industry. Thus, monitoring of water condensation modes on such interfaces under controlled conditions is of great importance towards the development of new functional surfaces enabling dropwise condensation. The water condensation chamber reported here is an easy to build and handle unit, that allows the study of such materials or surfaces under stable, repeatable conditions with concomitant monitoring of condensation phenomena in small, lab-scale, without the need for large-scale constructions and samples. In the preliminary results collected during the evaluation of the unit operation performance on testing hydrophilic, hydrophobic and superhydrophobic specimens the device worked fine with excellent performance in its control variables such as low response time, deviation and variation. Information gathered during the preliminary tests run clearly provided evidence that a high contact angle is not the only perquisite for drop-wise condensation. It was observed that water may condensate in a film-wise manner on hydrophobic surfaces. Thus, indicating that in such cases further investigation on the effect of micro/nanoscale surface topography is required, in order to enlighten the various aspects of surface and condensate interaction, responsible for the removal of condensate droplets in a DWC mode.

Acknowledgements

This research has been co-financed by the European Regional Development Fund of the European Union and Greek national funds through the Operational Program Competitiveness, Entrepreneurship and Innovation, under the call "Special Actions AQUACULTURE – INDUSTRIAL MATERIALS – OPEN INNOVATION IN CULTURE" (project code: T6YBP-00350) and this work has received funding from the European Union's Horizon 2020 research and innovation programme under grant agreement No 958274

References

[1] H. Jouhara, N. Khordehgah, S. Almahmou, B. Delpech, A. Chauhan, S. A. Tassou, Waste heat recovery technologies and applications, Therm. Sci. Eng. Prog. 6 (2018) 268-289.

[2] H. Chen, Y. Zhou, S. Cao, X. Li, X. Su, L. An, D. Gao, Heat exchange and water recovery experiments of flue gas with using nanoporous ceramic membranes, Applied Thermal Engineering 110 (2017) 686-694.

[3] C.M. Duron, J. Zhong, A.E. David, W.R. Ashurst, S.H. Bhavnani, J.R. Morris, A.C. Bates, Development of a durable vapor phase deposited superhydrophobic coating for steam cycle power generation condenser tubes, American Society of Mechanical Engineers V001T005A003-V001T005A003 (2017).

[4] Q. Zhuang, P. Geddis, B. Clements, V. Ko, Corrosion-resistant coating development with potential application in equipment of low-temperature waste heat recovery, The Canadian Journal of Chemical Engineering 96 (2018) 101-106.

[5] K. Rykaczewski, A.T. Paxson, M. Staymates, M.L. Walker, X. Sun, S. Anand, S. Srinivasan, G.H. McKinley, J. Chinn, J.H.J. Scott, Dropwise condensation of low surface tension fluids on omniphobic surfaces Scientific reports 4 (2014) 4158.

[6] S.Q. Cai, A. Bhunia, Superhydrophobic condensation enhanced by conical hierarchical structures. The Journal of Physical Chemistry C121 (2017) 10047-10052.

[7] V. Stathopoulos, V. Sadykov, S. Pavlova, Y. Bespalko, Y. Fedorova, L. Bobrova, A. Salanov, A. Ishchenko, V. Stoyanovsky, T. Larina, V. Ulianitsky, Z. Vinokurov, V. Kriventsov, Design of functionally graded multilayer thermal barrier coatings for gas turbine application, Surface and Coatings Technology 295 (2016) 20-28.

[8] P. Nanou, A. Zarkadoulas, P.K. Pandis, I. Tsilikas, I. Katis, D. Almpani, N.G. Orfanoudakis, N. Vourdas, V.N. Stathopoulos, Micromachninig on stainless steel 304 for improved water condensation properties (Proceedings of MSSM2022, 11-13 July 2022, Brunel University London-UK) Key Engineering materials, 2023 "accepted"

[9] P. Nanou, J. Konstantaras, A. Zarkadoulas, V.N. Stathopoulos, Development and evaluation of corrosion resistance hydrophobic properties of thermal sprayed coatings over carbon steel, MSSM2022 (Proceedings of MSSM2022, 11-13 July 2022, Brunel University London-UK) Key Engineering materials, 2023 "accepted"

[10] N. Vourdas, E. Marathoniti, P.K. Pandis, C.Argirusis, G. Sourkouni, C. Legros, S. Mirza, V. N. Stathopoulos, Evaluation of $LaAlO_3$ as top coat material for thermal barrier coatings, Trans. Nonferrous Met. Soc. China 28 (2018) 1582−1592.

[11] V. Kovalenko, V. Kotok, V.N. Stathopoulos, Smart Coatings Against Corrosion. Encyclopedia of Smart Materials 1 (2022) 400-413.

[12] S. Adera, L. Naworski, A. Davitt, N. K. Mandsberg, A. V. Shneidman, J. Alvarenga, J. Aizenberg, Enhanced condensation heat transfer using porous silica inverse opal coatings on copper tubes Sci. Rep. 11 (2021) 10675.

[13] N. Vourdas, H. Jouhara, S. A. Tassou, V. N. Stathopoulos, Design criteria for coatings in next generation condensing economizers, Energy Procedia 161 (2019) 412–420.

[14] Z. Li, Y. Lu, R. S. Huang, J. Chang, X. Yu, R. Jiang, X. Yu, A. Roskilly, Applications and technological challenges for heat recovery, storage and utilisation with latent thermal energy storage, Applied Energy 283 (2021) 116277.

[15] D.J. Preston, D.L. Mafra, N. Miljkovic, J. Kong, E.N. Wang, Scalable graphene coatings for enhanced condensation heat transfer. Nano letters 15 (2015) 2902-290.

[16] L. Montorsi, H. Jouhara, M. Venturelli, B Delpech, I. Celades Lopez, M-G. Asci, G. Bright, G. Jacomelli, D. Kroll, L, Zacares, M. Manfredini, D. Turesson, E. Rubion, V. Stathopoulos, R. Poskas, W. Gernjak, J. Santos, I. Marin, T. Stepisnik, D. Iatrou, A.Sayegh, "iWAYS - Recycling of heat, water and material across multiple sectors: ceramic, chemical and steel industry, (Proceedings of MSSM2022, 11-13 July 2022, Brunel University London-UK) Key Engineering materials, 2023 "accepted"

[17] P. K. Pandis, S. Papaioannou, V. Siaperas, A. Terzopoulos, V. N. Stathopoulos, "Evaluation of Zn- and Fe- rich organic coatings for corrosion protection and condensation performance on waste heat recovery surfaces", Int. J. Thermofluids 3–4 (2020) 100025.

[18] I. Iliopoulos, A. Karampekios, P.K. Pandis, N. Vourdas, H. Jouhara, S. Tassou, V.N. Stathopoulos, Evaluation of organic coatings for corrosion protection of condensing economizers, Procedia Structural Integrity 10 (2018) 295-302.

[19] N. Vourdas, G. Pashos, G. Kokkoris, A.G. Boudouvis, V.N. Stathopoulos, Droplet mobility manipulation on porous media using backpressure. Langmuir 32 (2016) 5250-5258.

[20] J. Trosseille, A. Mongruel, L. Royon, M. G. Medici, D. Beysens, Roughness-enhanced collection of condensed droplets Eur. Phys. J. E 42 (2019) 144.

[21] J. Shim, D. Seo, S. Oh, J. Lee, Y. Nam, Condensation Heat Transfer Performance of Thermally Stable Superhydrophobic Cerium Oxide Surfaces, ACS Appl. Mater. Interfaces 10 (2018) 31765–31776.

Figure 5. (continued)

[22] C. A. Harper, E. M. Petrie, Plastics materials and processes: a concise encyclopedia., John Wiley & Sons, 2003, pp. 8-9.

[23] M. Psarski, J. Marczak, G. Celichowski, G. B. Sobieraj, K. Gumowski, F. Zhou, W. Liu, Hydrophobization of epoxy nanocomposite surface with 1H,1H,2H,2H-perfluorooctyltrichlorosilane for superhydrophobic properties, Cent. Eur. J. Phys. 10 (2012) 1197-1201.

[24] N. Vourdas, C. Ranos, V.N. Stathopoulos, Reversible and dynamic transitions between sticky and slippery states on porous surfaces with ultra-low backpressure, RSC Advances 5 (2015) 33666-33673.

[25] A. Milionis, C. Noyes, E. Loth, I. S. Bayer, A. W. Lichtenberger, V. N. Stathopoulos, N. Vourdas, Water-Repellent Approaches for 3-D Printed Internal Passages Materials and Manufacturing Processes 31 (2016) 1162-1170.

[26] N. Vourdas, K. Dalamagkidis and V. N. Stathopoulos, Active porous valves for plug actuation and plug flow manipulation in open channel fluidics, RSC Advances 5 (2015) 104594-104600.

[27] V. Chalkia, N. Tachos, P.K. Pandis, A. Giannakas, Maria K. Koukou, M.Gr. Vrachopoulos, L. Coelho, A. Ladavos, V.N. Stathopoulos, Influence of organic phase change materials on the physical and mechanical properties of HDPE and PP polymers, RSC Advances 8 (2018) 27438-27447.

[28] A. Goswami, S. C. Pillai, G. McGranaghan, Surface modifications to enhance dropwise condensation, Surfaces and Interfaces, 25 (2021) 101143.

Figure 6. (continued)

2.6. Micromachining on Stainless Steel 304 for Improved Water Condensation Properties, https://doi.org/10.4028/p-FwZKv7

Microstructure fabrication and chemical surface functionalization with low-surface-energy materials are the key steps to achieve hydrophobic surfaces with high water droplet contact angles (CA). In this work we employed wire Electric Discharge Machining (EDM) as a way to induce microstructure topography on stainless steel 304 coupons. The resulting topography was rendered hydrophobic using trichloro-1H,1H,2H,2H-perfluorooctyl silane (PFOTS) via gas phase deposition. The channels created by machining and PFOTS functionalization facilitate water condensation by increasing nucleation sites and enhancing droplet coalescence. The resulting surface is hydrophobic (CA~140^{o}) in contrast to the bare stainless steel 304, which is hydrophilic (CA~76^{o}). [56]
The comprehensive edition of this publication can be found in Figure 3.

Key Engineering Materials
ISSN: 1662-9795, Vol. 962, pp 19-26
doi:10.4028/p-FwZKv7

Submitted: 2022-07-26
Revised: 2023-01-13
Accepted: 2023-04-19
Online: 2023-10-12

Micromachining on Stainless Steel 304 for Improved Water Condensation Properties

Paraskevi Nanou[1,2,a], Athanasios Zarkadoulas[1,2,b], Pavlos K. Pandis[1,3,c], Ioannis Tsilikas[4,5,d], Ilias Katis[5,d], Despoina Almpani[5,d], Nikolaos Orfanoudakis[1,3,e], Nikolaos Vourdas[1,3,f], Vassilis Stathopoulos[1,3,g] *

[1]Laboratory of Chemistry and Materials Technology, Department of Agricultural Development, Agrofood and Management of Natural Resources, National and Kapodistrian University of Athens, Psachna Campus, 34400, Evia, Greece.

[2]University of Thessaly, Gaiopolis Campus – Ring Road of Larissa-Trikala, GR41500 Larissa Greece.

[3]NCSR "Demokritos", Institute of Nanoscience and Nanotechnology, POB 60228, 153 10 Agia Paraskevi, Attiki, Greece.

[4]Physics Department, National Technical University of Athens, Zografou Campus, 15780 Athens, Greece.

[5]Cos Hellas Ltd, Mechanical Workshop, Palaion Faliro, 17564, Athens, Greece,

[a]nanoupar@uoa.gr, [b]azarkadoulas@uoa.gr, [c]ppandis@uoa.gr, [d]info@coshellas.com , [e]norfan@uoa.gr, [f]n.vourdas@inn.demokritos.gr, [g]vasta@uoa.gr

Keywords: coatings, condensation, stainless steel, surface roughness, micromachining

Abstract. Microstructure fabrication and chemical surface functionalization with low-surface-energy materials are the key steps to achieve hydrophobic surfaces with high water droplet contact angles (CA). In this work we employed wire Electric Discharge Machining (EDM) as a way to induce microstructure topography on stainless steel 304 coupons. The resulting topography was rendered hydrophobic using trichloro-1H,1H,2H,2H-perfluorooctyl silane (PFOTS) via gas phase deposition. The channels created by machining and PFOTS functionalization facilitate water condensation by increasing nucleation sites and enhancing droplet coalescence. The resulting surface is hydrophobic (CA~140°) in contrast to the bare stainless steel 304, which is hydrophilic (CA~76°).

Introduction

Waste heat recovery from low temperature heat streams (bellow 200°C) may contribute significantly to the improvement of energy efficiency of processes in various industrial sectors [1,2]. This recovery of waste heat is technically feasible through various technologies able to generate valuable energy sources, thus reducing the overall energy consumption and providing opportunities for energy optimisation in the steel and iron, food, and ceramic industries. Among the numerous technologies such as regenerators, recuperators, regenerative and recuperative burners, passive air preheaters, plate heat exchangers and economisers and waste heat boilers etc [1, 2]. In most cases recovery is achieved via condensation. Thus, significant energy savings and consequently substantial greenhouse gas emission reductions can be achieved by exploiting the condensation latent heat of the flue gases of such low temperature heat streams by using condensing economizers and pertinent facilities. In various processes, varying modes of condensation can result in significant amounts of heat as well as water recovery.

During the past years surface processing and engineering has provided tools towards solutions for additional favourable surface features related to wetting phenomena facilitating more efficient management of energy resources. Namely, enhancing dropwise condensation yields high heat transfer coefficients [1-4]. Such tools can enhance dropwise condensation over the film-wise condensation. Higher heat transfer rates are achieved because during film-wise condensation a water film is formed on the surface, which acts like a heat transfer barrier. In contrast, dropwise condensation mode

improves the surface renewal because the droplets slide-off and make room for more vapor to condense on the now free surface. They may also increase the rate of condensate collection or even generate alternative mechanisms of condensates removal from heat recovery surfaces such as self-jumping. In all cases the result is a tremendous improvement on the heat transfer coefficient and hence on the thermal efficiency of related heat exchange and recovery applications.

In the delicate interplay of water condensation and droplet departure, hydrophobic surfaces may facilitate this process. However, the hampered heat transfer at the initial state of droplet nucleation due to the insulating effects of hydrophobic coatings can lead to inefficient water condensation and departure from the surface [3-6]. Apart from condensation rate on a cooled surface, water collection rate is also important and a way to force droplet coalescence is via microgrooves i.e., introducing a favourable microstructure and/or topography on the steel surface [7,8].

There is a variety of machining techniques which are developed for micro-texturing on different materials and free-form surfaces [9], such as Laser Machining [9,10] and Wire Electric Discharge Machining (EDM) [11,12]. EDM is a manufacturing procedure where the electric discharge between a wire (electrode) and a work piece (conductive material) is used in order to remove certain amount of material from the work piece. Using this principle and configuring the parameters evolved, such as wire – piece distance, voltage, conductivity etc., it is possible to form any conductive raw material and determine its final shape with very little deviations from the desired nominal geometry, thus achieving high dimensional tolerances. These tolerances can reach up to a few micrometres.

Recent studies report that microstructure fabrication using machining techniques and further silane-modification can lead on hydrophobic surfaces [9-13]. In the present study EDM was employed as a convenient method to induce two different microstructure patterns on stainless steel 304 coupons in order to compare their performance under the same conditions. Coupons were rendered superhydrophobic by applying trichloro-1H,1H,2H,2H-perfluorooctyl silane, (PFOTS) via gas phase deposition. The channels created by machining facilitate water condensation and PFOTS coating enhances droplet coalescence via hydrophobicity. Such surface modifications lead to surfaces with lower surface energy [8] and enhanced oxidation-resistant properties, combined with water repellency for anti-corrosion properties. Grooves on stainless steel surface can contribute to a long-range coalescence mechanism over the metal surface, with accelerated water collection rates, overcoming the limitations posed by application of often non-homogeneous hydrophobic smooth surfaces.

Experimental

Sample preparation. Introduction of Roughness-Microstructure.

The workpieces were 304 stainless steel blocks with sizes of 2.9 cm × 2.9 cm × 2 mm. The substrates were obtained by wire EDM with circular geometry wire. Topography patterns at one or two planar directions were created.

The fabrication procedure for every coupon is the same and consists of the following basic steps. Figure 1 depicts schematically the steps described.

1. Initializing: Finding the surface of the work piece by contact ("touching" it). This is the point in space where electric discharge takes place between the wire and the piece.
2. Setting the origin: The measured distance is saved by the machine and is used as the reference plane. Cutting depth is defined in relevance to this plane.
3. Cutting: Wire is moved towards the workpiece (Y movement) as the input cutting depth parameter is set.
4. Retracting: Wire is retracted back at a safe distance.
5. Moving: Wire is moved along the perpendicular axis (X or Z – movement) as the pitch parameter is set.
6. Repeating steps 3 – 5.

Figure 3. Comprehensive edition of "Micromachining on Stainless Steel 304 for Improved Water Condensation Properties"

Different results occur for different pitch, cutting depth as well as current parameters. For the same current parameters and same work piece material the cutting parameters per case are summarized in Table 1:

Table 1. Benchmarking results

Coupon	X – Pitch (µm)	Z – Pitch (µm)	Y – Cutting Depth (µm)
1	350	0.35	7
2	350	none	10

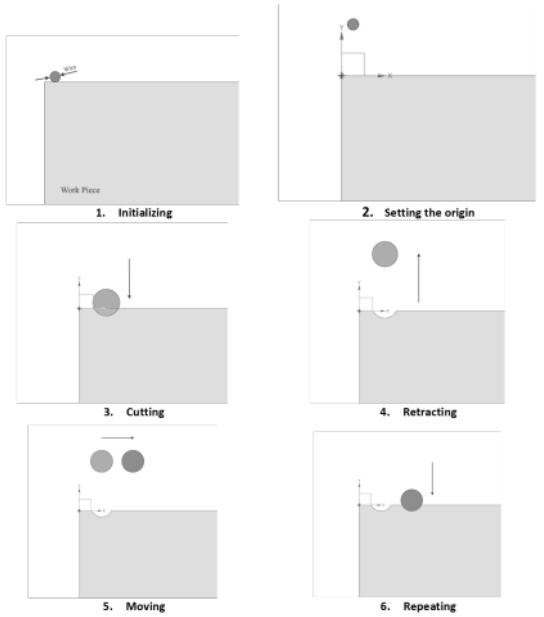

Figure 1. Steps described and nominal resulting geometry (Cross sectional view).

Chemical surface functionalization. In order to render samples hydrophobic, the following procedure was followed. The coupons were thoroughly degreased in soapy water, rinsed with doubly distilled water, ethanol, and acetone, and oven dried at 50 °C for 10 min. The clean and dry surfaces were initially treated by immersing the coupons in 1 M H_3PO_4 solution for 10 min at room temperature, washing with doubly distilled water, and oven drying at 50 °C for 10 min. The specimen was then coated with a superhydrophobic silane (trichloro-1H,1H,2H,2H-perfluorooctyl)silane, PFOTS) 10% v/v in hexane, via gas phase deposition as described before [14-17].

Sample Characterization. SL200 KS optical contact angle meter from Kino was used to measure surface wettability at room temperature applying Young-Laplace fitting method [17, 18]. The water droplet had volume equal to 10 µL. Condensation phenomena were recorded under 80% Relative Humidity (RH) at 30 °C in a custom-made water condensation chamber. [19] The specimen surface was maintained at 10 °C using a Peltier module. Prior to any measurement coupons were oven dried at 50 °C for 10 min.

Results and Discussion

Resulting surface pattern. Fig. 2 and Fig 3. show the resulting surface pattern is either one – directional canals for coupon 2 or pyramidal structures that occur from the junction of the two – directional canals for case 1.

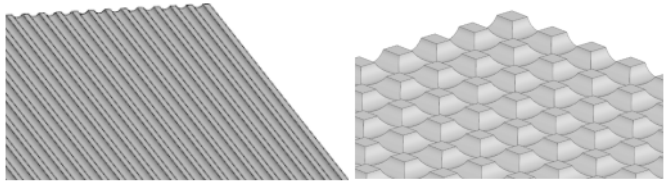

Figure 2. Resulting geometry of coupons after EDM. Top: one-directional canals; bottom: pyramidal structures.

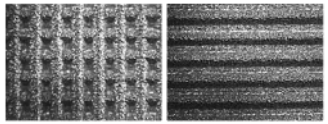

Figure 3. Optical microscope (5x) photos of clean coupons: 1 (left) and 2.

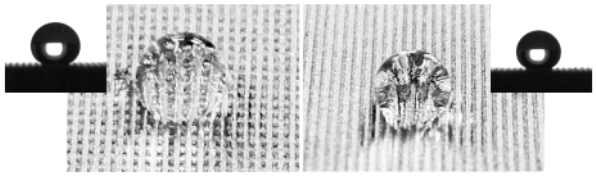

Figure 4. CA of water droplets on SS304, PFOTS-functionalized coupons: 1 (left) and 2 (right).

Figure 3. (continued)

Contact Angle (CA). Contact angle measurements revealed all steel samples become superhydrophilic prior to functionalization and after H_3PO_4 treatment, indicating successful preparation of the surface for strong, covalent attachment of silane moiety. Studies on the phosphoric acid etching of steel alloys [20] indicates that H_3PO_4 induces the emergence of Cr, Ni, and Mo on steel surface, providing thus anchoring points for strong, covalent attachment of PFOTS on the modified steel surface. SS 304 and coupons 1 and 2 become hydrophobic after PFOTS functionalization in contrast to initial SS 304 which was hydrophilic (76°). Specifically, SS 304 after PFOTS without machining became hydrophobic with CA 120°. As shown in Figure 4 Coupon 1 and Coupon 2 became high hydrophobic with CA reaching ~140 °. These results indicate that machining enhances the surface hydrophobicity. Results of CA measurements for each coupon are summarized below (Table 2).

Table 2. Contact angles

Coupon	CA (deg)
SS304	76.0 ± 0.5
SS304 (PFOTS)	120.2 ± 5.0
Coupon 1	138.4 ± 16.6
Coupon 2 (parallel)	146.7 ± 7.0
Coupon 2 (perpendicular)	138.6 ± 3.4

Water Condensation. Contact angle measurements provide quantitative information of the surface wettability. However, in order to study the mode of water condensation on the surface, it is important to study the condensation phenomena. In general, CA measurement can provide preliminary insight on whether a surface can be employed for water condensation. However, a high contact angle is not the only parameter that results in drop-wise condensation. In this work, water condensation in an 80% RH environment reveals the effect of micromachining on water condensation and droplet coalescence. On bare SS304, filmwise condensation is observed, with the formation of a continuous liquid film on the coupon surface as shown in Fig. 5. After surface functionalization with PFOTS, it becomes evident that droplets start forming and coalescing after 10 and 30 min of exposure in the humid environment. After 60 min, the formed droplets already flow due to gravity.

On coupon 1, dropwise condensation occurs in the first 30 min and droplet size after 60 min increases significantly, owing to the crosshair pattern of the coupon, indicating the positive effect of micromachining on water condensation and eventually water collection. In the case of coupon 2, dropwise condensation becomes again evident after 30 min of exposure, but in contrary to coupon 1, the size evolution and the degree of droplet coalescence is smaller in this case but significantly better than SS304 (PFOTS). Both cases indicating the improved performance of SS304 with EDM induced topography as well as surface functionalization by PFOTS. This is in good agreement with other reports on surface groove modifications [8] despite the different dimensions of the induced topography. These findings indicate that an induced topography by means of surface engineering over a heat exchange interface may have a positive effect in heat transfer. A detailed study is required.

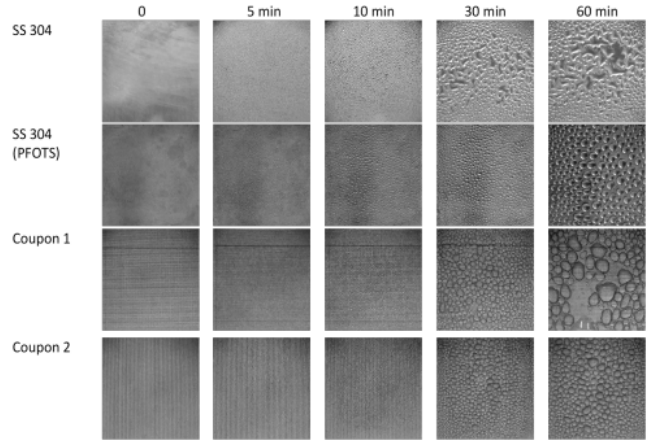

Figure 5. Water condensation on all samples mentioned in the present study (0, 5, 10, 30, 60 min).

Concluding Remarks

In this work, we successfully demonstrated the way in which micromachining of stainless steel 304 with Wire EDM and subsequent PFOTS surface modification can lead to an improved condensation performance as well as mobility of droplets. Considering that droplets are not pinned, improved water collection rates may be expected. However, water collection rates were not reported in this work. Although a hydrophobic surface contributes positively to dropwise condensation, introduction of surface roughness can further enhance water condensation, droplet coalescence, and water flow through microchannels with the ultimate goal of increased water collection rates, and consequently heat recovery. In this study Wire EDM induced topography of pyramidal structures formed by cutting curved channels of 350 x 70 x 350 μm and subsequent PFOTS modification of 304 steel surface resulted in surfaces that under condensation conditions showed improved water droplets formation and droplets of higher mobility. These surfaces performed better than the respective non machined SS304 coupons being hydrophobic by only PFOTS functionalization. Such an approach seems promising for delivering surfaces of improved heat transfer properties in technologies such as condensing economisers and should be further studied.

Acknowledgements

This research has been co-financed by the European Regional Development Fund of the European Union and Greek national funds through the Operational Program Competitiveness, Entrepreneurship and Innovation, under the call "Special Actions AQUACULTURE – INDUSTRIAL MATERIALS – OPEN INNOVATION IN CULTURE" (project code:T6YBP-00350 and T6YBP00483).

Figure 3. (continued)

References

[1] H. Jouhara, N. Khordehgah, S. Almahmou, B. Delpech, A. Chauhan, S. A.Tassou, Waste heat recovery technologies and applications, Therm. Sci. Eng. Prog. 6 (2018) 268-289.

[2] L. Montorsi, H. Jouhara, M. Venturelli, B Delpech, I. Celades Lopez, M-G. Asci, G. Bright, G. Jacomelli, D. Kroll, L, Zacares, M. Manfredini, D. Turesson, E. Rubion, V. Stathopoulos, R. Poskas, W. Gernjak, J. Santos, I. Marin, T. Stepisnik, D. Iatrou, A.Sayegh, "iWAYS - Recycling of heat, water and material across multiple sectors: ceramic, chemical and steel industry", (Proceedings of MSSM2022, 11-13 July 2022, Brunel University London-UK) Key Engineering materials, 2022 "accepted".

[3] X. Hu, Q. Yi, X. Kong, J. Wang, A Review of Research on Dropwise Condensation Heat Transfer, Appl. Sci. 11 (2021) 1553.

[4] N. Vourdas, H. Jouhara, S. A. Tassou, V. N. Stathopoulos,Design criteria for coatings in next generation condensing economizers, Energy Procedia 161 (2019) 412–420.

[5] P.K. Pandis, S. Papaioannou, V. Siaperas, A. Terzopoulos, V. N. Stathopoulos, Evaluation of Zn- and Fe- rich organic coatings for corrosion protection and condensation performance on waste heat recovery surfaces, Int. J. Thermofluids 3–4 (2020) 100025.

[6] I. Iliopoulos, A. Karampekios, P.K. Pandis, N. Vourdas, H. Jouhara, S. Tassou, V.N. Stathopoulos, Evaluation of organic coatings for corrosion protection of condensing economizers, Procedia Structural Integrity 10 (2018) 295-302.

[7] J. Trosseille, A. Mongruel, L. Royon, M. G. Medici, D. Beysens, Roughness-enhanced collection of condensed droplets, Eur. Phys. J. E 42 (2019) 144.

[8] P.B. Bintein, H. Lhuissier, A. Mongruel, L. Royon, D. Beysens, Grooves Accelerate Dew Shedding, Phys. Rev. Let. 122 (2019) 098005.

[9] V. K. Jain, D. S. Patel, J. Ramkumar, B. Bhattacharyya, B. Doloi, B. R. Sarkar, P. Ranjan, S. Sankar E. S., A. D. Jayal, Micro-machining: An overview (Part II), J. of Micromanufacturing (2022) 46.

[10] Y. Cai, W. Chang, X. Luo, A. M. L. Sousa, K. H. A. Lau, Y. Qin, Superhydrophobic structures on 316L stainless steel surfaces machined by nanosecond pulsed laser, Precision Engineering (2018) 266.

[11] D. Cao, S. Ji, J. Zhao, Z. Liu, H. Dai, Design and superhydrophobic performance analysis of the rectangular-groove microstructure coated by nanocoatings, Mater. Chem. Phys. (2022) 126539.

[12] L. Ouyang, J. Liu, Y. Xiao, Y. Zhang, G. Xie, H. Zhang, Z. Yu, One-Step Preparation of a Superhydrophobic Surface by Electric Discharge Machining with a Carbon Fiber Brush Electrode, Langmuir (2022) 9853.

[13] C. Stamatopoulos, A. Milionis, N. Ackerl, M. Donati, P.L. de la Vallée, P. R. von Rohr, D. Poulikakos, Droplet Self-Propulsion on Superhydrophobic Microtracks, ACS Nano 14 (2020) 12895-12904.

[14] M. Psarski, J. Marczak, G. Celichowski, G. B. Sobieraj, K. Gumowski,F. Zhou, W. Liu, Hydrophobization of epoxy nanocomposite surface with 1H, 1H, 2H, 2H perfluorooctyltrichlorosilane for superhydrophobic properties, Cent. Eur. J. Phys. 10 (2012) 1197-1201.

[15] N. Vourdas, C. Ranos, V.N. Stathopoulos, Reversible and dynamic transitions between sticky and slippery states on porous surfaces with ultra-low backpressure, RSC Advances 5 (2015) 33666-33673.

[16] A. Milionis, C. Noyes, E. Loth, I. S. Bayer, A. W. Lichtenberger, V. N. Stathopoulos, N. Vourdas, Water-Repellent Approaches for 3-D Printed Internal Passages, Materials and Manufacturing Processes 31 (2016) 1162-1170.

[17] N. Vourdas, K. Dalamagkidis and V. N. Stathopoulos, Active porous valves for plug actuation and plug flow manipulation in open channel fluidics, RSC Advances 5 (2015) 104594-104600.

[18] V. Chalkia, N. Tachos, P.K. Pandis, A. Giannakas, M.K. Koukou, M. Gr. Vrachopoulos, L. Coelho, A. Ladavos, V.N. Stathopoulos, Influence of organic phase change materials on the physical and mechanical properties of HDPE and PP polymers, RSC Advances 8 (2018) 27438-27447.

[19] P. Nanou, J. Konstantaras, A. Zarkadoulas, P. K. Pandis, N. Vourdas, V.N. Stathopoulos, Construction, evaluation and performance of a water condensation test unit, (Proceedings of MSSM2022, 11-13 July 2022, Brunel University London-UK) Key Engineering materials, 2022 "accepted".

[20] K. Prabakaran, S. Rajeswari, Electrochemical, SEM and XPS investigations on phosphoric acid treated surgical grade type 316L SS for biomedical applications, J. Appl. Electrochem (2009) 887.

Figure 3. (continued)

2.7. Bioenergy Production from Tannery Waste via a Single-Chamber Microbial Fuel Cell with Fly Ash Cathodic Electrodes, https://doi.org/10.4028/p-0xWsyq

Microbial Fuel Cells (MFCs) are attracting attention for their application in simultaneous energy production and waste treatment, as innovative biochemical reactors. They usually operate under adiabatic conditions, utilizing microorganisms to treat wastewater compositions using mainly carbon-based electrodes as anodes and cathodes. During the past years, various anodic and cathodic electrodes with plenty of variations were used in MFC configurations. On the anode side metal-based electrodes are used while on the cathode, ceramic electrodes are currently introduced. In this study, a stainless steel anode is used in a single chamber MFC. Ceramic cathodic electrodes are used, coated with Fly Ash (FA). The mixed transition oxides of FA are tested as potential cathodic catalysts in the operation of the MFC. The FA powder was deposited by two methods: an ultrasound-assisted method and a conventional brush coating. Tannery liquid waste is used as the waste/substrate to be treated in the single-chamber MFC. The configuration with ultrasound-assisted Fly-Ash produced cathodic electrodes, led to the highest power output in batch operation modes and a high degree of simultaneous COD decrease of the tannery waste reaching the values of 0.44 mW/g_{cat} and 85.6% COD removal respectively. [65]

The comprehensive edition of this publication can be found in Figure 4.

Key Engineering Materials
ISSN: 1662-9795, Vol. 962, pp 105-112
doi:10.4028/p-0xWsyq
© 2023 Trans Tech Publications Ltd, Switzerland

Submitted: 2022-09-15
Revised: 2023-04-13
Accepted: 2023-04-19
Online: 2023-10-12

Bioenergy Production from Tannery Waste via a Single-Chamber Microbial Fuel Cell with Fly Ash Cathodic Electrodes

Pavlos K. Pandis[1,2,a*], Eleftherios Michopoulos[1,b], Charalambos Arvanitis[1,c], Christos Argirusis[1,d], Vassilis N. Stathopoulos[2,e], Gerasimos Lyberatos[1,3,f] and Asimina Tremouli[1,g]

[1] School of Chemical Engineering, Zografou Campus, National Technical University of Athens, 9 Heroon Polytechneiou St., 15780 Athens, Greece; ppandis@chemeng.ntua.gr

[2] Laboratory of Chemistry and Materials Technology, Department of Agricultural Development, Agrofood and Management of Natural Resources, National and Kapodistrian University of Athens, Psachna Campus, 34400, Evia, Greece.

[3] Institute of Chemical Engineering Sciences (ICE-HT), Stadiou St., Platani, 26504 Patras, Greece.

[a]ppandis@chemeng.ntua.gr, [b]lefterismichopoulos@gmail.com, [c]xaris.origin@gmail.com, [d]amca@chemeng.ntua.gr, [e]vasta@uoa.gr, [f]lyberatos@chemeng.ntua.gr, [g]atremouli@chemeng.ntua.gr

Keywords: Tannery waste; microbial fuel cell; fly ash ceramic electrodes; bioenergy; waste treatment

Abstract. Microbial Fuel Cells (MFCs) are attracting attention for their application in simultaneous energy production and waste treatment, as innovative biochemical reactors. They usually operate under adiabatic conditions, utilizing microorganisms to treat wastewater compositions using mainly carbon-based electrodes as anodes and cathodes. During the past years, various anodic and cathodic electrodes with plenty of variations were used in MFC configurations. On the anode side metal-based electrodes are used while on the cathode, ceramic electrodes are currently introduced. In this study, a stainless steel anode is used in a single chamber MFC. Ceramic cathodic electrodes are used, coated with Fly Ash (FA). The mixed transition oxides of FA are tested as potential cathodic catalysts in the operation of the MFC. The FA powder was deposited by two methods: an ultrasound-assisted method and a conventional brush coating. Tannery liquid waste is used as the waste/substrate to be treated in the single-chamber MFC. The configuration with ultrasound-assisted Fly-Ash produced cathodic electrodes, led to the highest power output in batch operation modes and a high degree of simultaneous COD decrease of the tannery waste reaching the values of 0.44 mW/g_{cat} and 85.6% COD removal respectively.

1 Introduction

Tannery is one of the oldest and most important industries in the world, especially for the countries around the Mediterranean [1]. However, tanneries are among the industries that produce the most hazardous waste, not only because of the use of toxic substances and compounds (tannins, sulfides, dyes, and various chemicals) but also because of the significant variations in their qualitative and quantitative characteristics from industry to industry. The differences are related to the size of the industry and the desired end result. The production process, the chemicals and the quantities of water used, have a direct effect on the final effluents, creating highly toxic wastewater that has to be treated. Main chemical properties of tannery waste to be monitored are the Chemical Oxygen Demand (COD), Biochemical Oxygen Demand (BOD), sulfates, pH and heavy metals (mainly Cr) [2, 3].

At a global level, research studies have been carried out towards suitable tannery wastewater treatment technologies. The most widely studied among them are advanced oxidation [4] and membrane processes [1], electrochemical [5, 6] and physicochemical treatment (such as flocculation) [7] and aerobic and anaerobic processes [8]. Because of the high levels of COD the biological treatment showed significant improvement when it follows a pre-treatment step, to make the waste more biodegradable [9].

Microbial Fuel Cells (MFCs) have been described as an economical, environmentally friendly and sustainable wastewater treatment technology [10, 11]. They can be advantageous over conventional treatment methods as they utilize the chemical energy of the wastewater to generate electricity while processing it, under anaerobic conditions. Complex organic municipal and industrial wastes have been successfully tested and demonstrated that MFCs are a promising alternative to conventional aerobic biological activated sludge treatment with associated economic benefits [12].

Tannery outflows have some features that have been shown to benefit the use of MFCs for their processing. One such factor is the acidic pH of the waste, which is crucial for Oxygen Reduction Reactions (ORR) in the cathode. In addition to the benefit of proton availability, acidic conditions also prevent methane-producing bacteria, whose populations act suppressively, blocking the largest number of electrons that would otherwise be directed to bio-anode. Thus, acidophilic conditions are ideal for the treatment of tannery waste using MFCs [13]. Another characteristic of tannery effluents is that endogenous waste bacteria, which survive the complex organic and sulfate compounds as well as the large variety of heavy metals, are a good source of electro-active bacteria for cultivation. The performance of MFCs is directly related to the type and suitability of the bacteria used and the biodegradation generated. A linear COD power/load dependence of up to 3000 – 6000 mg·COD/L has been reported, depending, of course, on the complexity of this load [14, 15]. Under that scope, urban and industrial wastewaters can potentially be seen as resources and not as barriers, an important factor in achieving an environmentally friendly and energy-efficient future.

An industrial waste that requires special attention and treatment and may fall (from a different perspective) into the above category is Fly Ash (FA). Derived from the combustion of carbon-rich fossil fuels in a variety of industrial applications, power plants but also from the combustion of solid waste (which is applied in several European countries), FA is one of the most complex and dangerous anthropogenic solid waste. It has to be noted, that studies have identified the existence of 316 different minerals from 188 mineral classes in various FA samples from across the world [16].

Disposal of FA quantities in landfills, open water tanks or their burial can cause enormous heavy metal pollution problems to the aquifer, groundwater, and soil. Their utilization is therefore considered to be of utmost importance for the maintenance of public health The literature on the utilization of FA has been extensively reported, in various applications, mainly in the field of construction and building materials and applications. The most common of those is the addition of cement up to 35% in cement [16, 17] depending on the application. There is also an attempt to create a binding geopolymer that will replace classic cement [18, 19], as well as the production of more durable ceramic building materials (modern bricks) [16, 20]. In addition to the above traditional applications, intense research has been reported in recent years on the use of FA in the fuel cell industry to produce more efficient electrodes [21] and polymeric electrolytic membranes [22]. Also, the simultaneous utilization of FA and sewage sludge has led to the construction of high-performance anodes for MFCs [23], while research effort is also expanding in the field of ion-lithium battery performance optimization, by adding a film of FA to the cathode [24]. FA is mainly consisted of metal oxides (eg. CaO, MnO, FexOy, Al_2O_3 etc) which may contribute to the overall operation in terms of enhancing the ORR in the cathode. These oxides, even in small quantities, may provide substantial yield to the overall performance of the MFC.

This study utilizes FA in a microbial fuel cell's cathode electrode and evaluates its performance in comparison to state-of-the-art electrodes using carbon-based materials. Two proposed ways of ceramic electrode fabrication are proposed based on previous studies and their performance results are presented in terms of energy production and waste degradation in a single chamber Microbial Fuel Cell.

2 Materials and Methods

All the materials used for the experiments were cost-efficient and available in the global market. An intermediate target of this study is to validate the usage of commercial materials in the design of an MFC whilst the production methods were chosen to be time and energy efficient. Reproducible electrode configurations were achieved in terms of catalyst (FA) loading in the cathode side of the

Figure 4. Comprehensive edition of "Bioenergy Production from Tannery Waste via a Single-Chamber Microbial Fuel Cell with Fly Ash Cathodic Electrodes"

MFCs. In order to estimate the FA content effect on the performance of the MFC three different loadings are presented below. Due to the fact that FA cannot be adhered to the support of the cathode of the MFC an acrylic binder was used in order to achieve a proper adhesive suspension precursor for the electrodes' preparation.

2.1 Materials

The test cathodic tubes were manufactured using commercial mullite tubes with dimensions of Ø25 mm x 100 mm, with an internal diameter of Ø20 mm, a useful internal catalyst surface of 0.31 m^2 and a total open porosity of 20%, calculated with Archimedes method. Inside, for the current collection, a stainless steel (SS) mesh was placed, part of which protruded at the top to make the installation of the wiring easier for the following electrochemical measurements. In the end, the conductive paste made of fly ash and an acrylic base binder (HSF54 – YSHIELD, Germany) was placed. Common steel felt was used as an anode electrode (Nimax – code type 0857, Greece). The dimensions of these electrodes were: Ø25 x 180 mm with an inner diameter of Ø20 mm and a useful internal catalyst surface of 0.44 m^2. The tannery waste that was fed to the fuel cell was the supernatant liquid of a settling tank from a Greek tannery with values of COD=3600g/L, pH=8.31 and conductivity=18.77 mS/cm^{-1}.

2.2 Ceramic Electrode Preparation

For the fabrication of ceramic-supported FA electrodes, suspensions of suitable properties have been prepared as follows:

The suspension's total solid content was 40% w/w in water. Quantities of HSF54 and FA were mixed with 40 ml of deionized water, with the aim of preparing suspensions with the following FA:HSF54 ratio of 90:10, 50:50 and 0:100. Cetyl Trimethyl Ammonium Bromide (CTAB) was initially added to the water, equal to 0.6% w/w of the FA [27] and stirred under heating until completely dissolved. The as-produced suspension was deposited on the inner surface of the test cathodic tubes with two different techniques [25]: A. Ultrasound assisted (Sono-Coat – SC) and B. Manually brushed (Brush-Coat – BC) as described below.

A. Using ultrasound (Sono-Coat – SC) (Figure 1): The mullite tubes were fitted to the ultrasound device (Vibra cell 750 – SONICS, USA) so that the tip of the device reached a depth of 1 cm from the upper surface of the mullite tube. A quantity of the suspension was placed inside the ceramic tube (one side capped) with the aid of a pipette. The ultrasonication lasted 20 min at 19% amplitude producing 14.2 kW power, during which suspension refills were needed, so its level in the test tubes remained the same. At the end of the process, the remained amount of suspension was removed, and the produced FA electrodes (9010SC, 5050SC and 0100SC) were allowed to dry at ambient air for 24h.

Figure 1. Setup of ultrasound-assisted deposition (left) and Tube before and after ultrasound-assisted of HSF54 and Fly Ash deposition (right).

B. Manually brushed (Brush-Coat – BC): The suspension of HSF54 and FA was applied on the inner walls of the ceramic tube using a brush (size 4 – Germany) in 2 layers followed by drying at ambient air in between. The produced FA electrodes (9010BC, 5050BC and 0100BC) were also left to dry in ambient air for 24h.

2.3 Analytical methods and calculations

The COD, conductivity and pH value of the tannery waste were measured prior and after batch operation cycles of the cells. For this purpose, pH and conductivity were recorded using a digital pH-meter and a conductivity meter with pH sensor (SEN0161) and conductivity sensor (DFR0300-H) modules purchased from DFRobot, China, while the COD measurements were carried out according to standards as reported recently [25].

2.4 Electrochemical Characterization of cells

The electrochemical characterization of the cells included Open Current Voltage (OCV), Polarization Curves and Electrochemical Impedance Spectroscopy (EIS) in a single chamber Microbial Fuel cell with the two types of produced electrodes. More particular, the polarization curves were calculated from OCV to 0 V with a descent rate of 0.3 mV/s, while the EIS spectra ranged from 200 kHz to 10 mHz with an amplitude of 10 mV (sinusoidal). Acclimation cycles were conducted prior to the use of tannery waste with synthetic glucose with the same electrodes as reported elsewhere [25, 26]. All operation cycles on the cells were tested in batch mode anaerobically and the final accepted values were acquired as the mean value of three different measurements. A small-scale custom-made cell was constructed out of Ertalon material as shown in Figure 2. In each batch operation cycle, the waste composition was diluted to the values of COD=1020g/L, pH=7.67 and conductivity=12.15 mS/cm^{-1}.

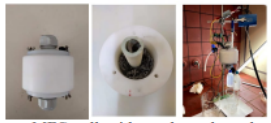

Figure 2. Batch operation setup MFC cell with steel anode and ceramic supported HSF54+FA cathodic electrode

3 Results

The results on the produced MFC configurations are presented below. Both techniques used for cathode preparation provided facile ways of utilizing FA as a cathodic catalyst in MFCs. Electrochemical characterization results ensured the proper investigation of the performance of different MFCs configurations. Especially the electrochemical techniques, presented in this study, provided a powerful tool for comprehending the processes onto the electrodes. Analytical techniques also provided results that allowed the proper correlation and comparison of the different MFC assemblies.

3.1 Ceramic-supported electrodes production

After the deposition of the cathodic catalyst onto the inner area of the ceramic mullite tubes, the catalysts quantities over the prepared electrodes with both brush and ultrasound techniques are depicted in Table 1. For comparison reasons, the final catalyst loading was maintained in the value of 1.51 ± 0.02 g for both MFC configurations.

Table 1. Final FA and HSF54 mass loadings on final produced electrodes

Deposition method	**BC**			**SC**		
ratio (FA:HSF54)	0:100	50:50	90:10	0:100	50:50	90:10
Code name	0100BC	5050BC	9010BC	0010BC	5050SC	9010SC
Final catalyst loading (g)	1.49	1.51	1.49	1.52	1.51	1.53

Although different initial suspensions may provide different catalyst loadings, both techniques were optimized for the loading of 1.51 ± 0.02 g of catalyst.

Figure 4. (continued)

3.2 Electrochemical Characterization of MFCs with produced fly ash cathodic electrodes

The batch operation cycles are depicted in Figure 3. Solid lines represent the polarization curves of the cells with the associated electrodes whilst dashed lines are attributed to power curves depicting the maximum power generation per catalyst mass produced. Table 2 provides a numeric representation of the maximum power output per sample and COD removal of the waste.

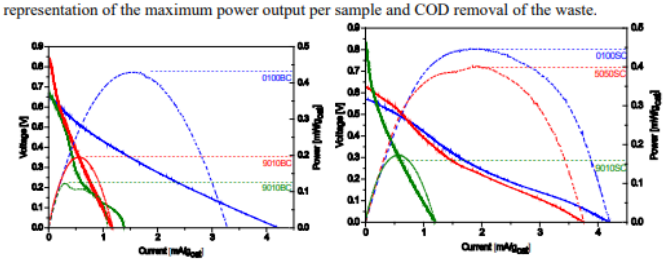

Figure 3. Polarization (solid lines) and power curves (dashed lines) for all the produced electrodes in batch operation modes

Table 2. Maximum power output and COD removal at different MFC configurations

Electrodes	0100BC	5050BC	9010BC	0100SC	5050SC	9010SC
Power (mW/g_{cat})	0.42	0.19	0.12	0.48	0.44	0.17
COD removal [%]	70.2	82.4	75.6	75.5	85.6	78.4

It is obvious that the ultrasound-assisted technique provided electrodes with an enhanced ability to produce more power and COD removal capacity of the tannery waste than the brush-coated ones. Taking into consideration that the quantity of the cathodic catalysts was practically the same, it is deducted that this method provided better electrodes for power generation from tannery waste. Although the electrodes with no FA content show the highest power output, 5050SC samples can produce also high or even satisfactory values of power ca 80% of the 0100SC power output and 5050BC samples ca. 46% of the 0100BC samples respectively. However, the FA introduction results in improved COD removal most probably through a synergy effect of the metal oxides of FA and the HSF54 binder that needs further study. The later can be further solidified due to the fact that a high content of FA in the electrodes is not increasing further the COD removal performance. Thus a high content of FA may be blocking current passages thus providing low power output and a higher COD removal.

Regarding the electrochemical values from EIS experiments [27], the values of the solution resistance (R_s), the biofilm resistance (R_{BF}), the charge transfer resistance (R_{CT}) of the cells also explain the behaviour are depicted in Table 3. 0100 electrodes have enhanced R_{CT} which verifies the high current blockage while R_{BF} is also lower in the cells with 0100 electrodes. The R_S is practically stable for all the cell configurations and is mainly associated with the waste composition.

Table 3. Calculated Values of EIS experiments

Microbial Fuel Cells with						
Fitted Parameters	0100BC	5050BC	9010BC	0100SC	5050SC	9010SC
R_S (Ω)	23.5	23.2	23.4	22.5	22.4	22.6
R_{BF} (Ω)	1.9	2.9	2.8	2.1	2.5	2.4
R_{CT} (Ω)	1.3	0.3	0.4	0.9	0.2	0.2

Taking into consideration the above results, it is obvious that the MFC configurations with brush-coated electrodes presented enhanced polarization in comparison with sono-coated. The main polarization of the brush-coat fuel cell configurations is attributed to ohmic losses in the 0100BC and 5050BC cases whilst in the case of 9010BC the curve of Figure 3 presented an initial slope of activation loss. On the other hand, all three (0100SC, 5050SC and 9010SC) fuel cell configurations provided results with clear ohmic losses (Figure 3) as the lines of polarization curves could be considered linear. The above considerations and interpretations are verified mainly through the values of R_{CT} as it was calculated lower in the case of sono-coated configurations. As this study is focused on the nature of the cathodic catalyst (FA), further research on optimizing the performance of the MFCs should be focused on mixtures of FA with different conductive polymers, different solid content of the suspensions or in different MFC cathodic supports with controllable porosity and different catalyst loading. Finally, different anodes may provide different results in terms of COD reduction and energy output due to the fact that metallic anodes are not so favoured in MFCs [6,7,10]. In terms of pH and conductivity, at first the tannery had a pH=5.0 and a conductivity of 14.3 mS/cm. All the above configurations resulted in a pH value of 7.6 while the conductivity results varied. In the case of brush-coated configurations the conductivity dropped at 10.4 mS/cm and in the case of sono-caoted maintained the value of 13.5 mS/cm. The drop of the conductivity in both configurations was expected due to the fact of utilizing the conductive species of the anodic solution. In the case of brush-coated configurations the lower conductivity signified the higher ohmic loss as verified by both polarization and EIS experiments.

4 Conclusions

In this work, two different coating techniques were applied to produce FA electrodes for power production from tannery waste. The technique of ultrasound provides more stable electrodes capable of treating MFCs with tannery waste. The internal resistances of the MFCs, operated in batch modes, are lower with the ultrasound technique verifying and solidifying the results on power curves. Although the power output is larger with no FA content, the ultrasound technique provided electrodes with capabilities of higher power output and COD removal than the brush coated. The electrodes' composition with FA and HSF54 in the same content enhnanced the power output and COD removal of the MFCs. The synergetic operation of HSF54 and FA is maximized in this composition. This indicates a practical and efficient strategy of implementing FA as cathodic catalyst in the MFC technology. The use of a conductive additive such as HSF54 is essential for the proper adhesion onto supported electrodes. It is clear that the FA is acting only as the catalyst for ORR whilst HSF54 provided a dual role both as catalyst and the electron acceptor. The use of FA as a cathodic catalyst in MFCs opens a new way for its utilization in energy production with simultaneous tannery waste treatment. Nevertheless, this research has to be optimized through different production strategies and materials selection and compositions substituting HSF54 and also including the major effect of different anode selection.

Acknowledgements

This project has been partially funded by the Hellenic Foundation for Research and Innovation (HFRI) and the General Secretariat for Research and Technology (GSRT), under grant agreement No [862].

Figure 4. (continued)

References

[1] R. Suthanthararajan, E. Ravindranath, K. Chits, B. Umamaheswari, T. Ramesh, S. Rajamam, Membrane application for recovery and reuse of water from treated tannery wastewater, Desalination, 164 (2004) 151-156.

[2] C. Di Iaconi, A. Lopez, R. Ramadori, A.C. Di Pinto, R. Passino, Combined chemical and biological degradation of tannery wastewater by a periodic submerged filter (SBBR), Water Research, 36 (2002) 2205-2214.

[3] S.G. Schrank;, U. Bieling;, H.J. José;, R.F.P.M. Moreira;, H.F. Schröder, Generation of endocrine disruptor compounds during ozone treatment of tannery wastewater confirmed by biological effect analysis and substance specific analysis, Water Science & Technology, 59 (2009) 31-38.

[4] T.P. Sauer, L. Casaril, A.L.B. Oberziner, H.J. José, R.d.F.P.M. Moreira, Advanced oxidation processes applied to tannery wastewater containing Direct Black 38—Elimination and degradation kinetics, Journal of Hazardous Materials, 135 (2006) 274-279.

[5] C.R. Costa, C.M.R. Botta, E.L.G. Espindola, P. Olivi, Electrochemical treatment of tannery wastewater using DSA® electrodes, Journal of Hazardous Materials, 153 (2008) 616-627.

[6] L. Szpyrkowicz, S.N. Kaul, R.N. Neti, S. Satyanarayan, Influence of anode material on electrochemical oxidation for the treatment of tannery wastewater, Water Research, 39 (2005) 1601-1613.

[7] S. Haydar, J.A. Aziz, Coagulation–flocculation studies of tannery wastewater using combination of alum with cationic and anionic polymers, Journal of Hazardous Materials, 168 (2009) 1035-1040.

[8] S. Goswami;, D. Mazumder;p, Treatment of Chrome Tannery Wastewater by Biological Process - A Mini Review, International Journal of Environmental and Ecological Engineering, 7 (2013).

[9] G.Durai;, M. Rajasimman, Biological Treatment of Tannery Wastewater- A review, Journal of Environmental Science and Terchnology, 4 (2011) 1-17.

[10] L. Ezziat, A. Elabed, S. Ibnsouda, S. El Abed, Challenges of Microbial Fuel Cell Architecture on Heavy Metal Recovery and Removal From Wastewater, Frontiers in Energy Research, 7 (2019).

[11] T.H.J.A. Sleutels, A. Ter Heijne, C.J.N. Buisman, H.V.M. Hamelers, Bioelectrochemical Systems: An Outlook for Practical Applications, ChemSusChem, 5 (2012) 1012-1019.

[12] J.R. Trapero, L. Horcajada, J.J. Linares, J. Lobato, Is microbial fuel cell technology ready? An economic answer towards industrial commercialization, Applied Energy, 185 (2017) 698-707.

[13] K.-J. Chae, M.-J. Choi, K.-Y. Kim, F.F. Ajayi, W. Park, C.-W. Kim, I.S. Kim, Methanogenesis control by employing various environmental stress conditions in two-chambered microbial fuel cells, Bioresource Technology, 101 (2010) 5350-5357.

[14] T. Kamperidis, P.K. Pandis, C. Argirusis, G. Lyberatos, A. Tremouli, Effect of Food Waste Condensate Concentration on the Performance of Microbial Fuel Cells with Different Cathode Assemblies, Sustainability, 14 (2022) 2625.

[15] G. Mohanakrishna, S. Venkata Mohan, P.N. Sarma, Bio-electrochemical treatment of distillery wastewater in microbial fuel cell facilitating decolorization and desalination along with power generation, Journal of Hazardous Materials, 177 (2010) 487-494.

[16] R.S. Blissett, N.A. Rowson, A review of the multi-component utilisation of coal fly ash, Fuel, 97 (2012) 1-23.

[17] D.P. Bentz, M.A. Peltz, A. Durán-Herrera, P. Valdez, C.A. Juárez, Thermal properties of high-volume fly ash mortars and concretes, Journal of Building Physics, 34 (2010) 263-275.

[18] M. Amran, S. Debbarma, T. Ozbakkaloglu, Fly ash-based eco-friendly geopolymer concrete: A critical review of the long-term durability properties, Construction and Building Materials, 270 (2021) 121857.

[19] S. Thokchom;, D. Dutta;, S. Ghosh;, Effect of Incorporating Silica Fume in Fly Ash Geopolymers, International Journal of Civil and Environmental Engineering, 5 (2011).

[20] X. Lingling, G. Wei, W. Tao, Y. Nanru, Study on fired bricks with replacing clay by fly ash in high volume ratio, Construction and Building Materials, 19 (2005) 243-247.

[21] M. Webster, H.Y. Lee, K. Pepa, N. Winkler, I. Kretzschmar, M.J. Castaldi, Investigation on electrical surface modification of waste to energy ash for possible use as an electrode material in microbial fuel cells, Waste Manag Res, 36 (2018) 259-268.

[22] G. Sivasubramanian, K. Hariharasubramanian, P. Deivanayagam, J. Ramaswamy, High-performance SPEEK/SWCNT/fly ash polymer electrolyte nanocomposite membranes for fuel cell applications, Polymer Journal, 49 (2017) 703-709.

[23] Y. Jia, H. Feng, D. Shen, Y. Zhou, T. Chen, M. Wang, W. Chen, Z. Ge, L. Huang, S. Zheng, High-performance microbial fuel cell anodes obtained from sewage sludge mixed with fly ash, Journal of Hazardous Materials, 354 (2018) 27-32.

[24] E.R. Dyartanti, A. Jumari, A. Nur, A. Purwanto, Improving lithium-ion battery performances by adding fly ash from coal combustion on cathode film, AIP Conference Proceedings, 1710 (2016) 030004.

[25] P.K. Pandis, T. Kamperidis, K. Bariamis, I. Vlachos, C. Argirusis, V.N. Stathopoulos, G. Lyberatos, A. Tremouli, Comparative Study of Different Production Methods of Activated Carbon Cathodic Electrodes in Single Chamber MFC Treating Municipal Landfill Leachate, Applied Sciences, 12 (2022) 2991.

[26] A. Tremouli, P.K. Pandis, I. Karydogiannis, V.N. Stathopoulos, C. Argirusis, G. Lyberatos, Operation and Electro(chemical) characterization of a microbial fuel cell stack fed with fermentable household waste extract, Global NEST Journal, 21 (2019) 253-257.

[27] X. Dominguez-Benetton, S. Sevda, K. Vanbroekhoven, D. Pant, The accurate use of impedance analysis for the study of microbial electrochemical systems, Chemical Society Reviews, 41 (2012) 7228-7246.

Figure 4. (continued)

2.8. Development and Evaluation of Corrosion Resistance and Hydrophobic Properties of Thermal Sprayed Coatings over Carbon Steel, https://doi.org/10.4028/p-sth09H

Various industrial parts and equipment made of steel need to withstand demanding conditions. In order to increase performance and lifetime, surface processing and functional coatings can be applied. In this study we report on the evaluation of coated carbon steel with commercial corrosion-resistant powders Diamalloy 4276 and Woka 7502 by Oerlikon Metco, using thermal spraying. Further functionalization is performed by rendering thermal sprayed surfaces syperhydrophobic via gas phase deposition of trichloro-1H,1H,2H,2H-perfluorooctyl silane, (PFOTS). Electrochemical impedance spectroscopy, contact angle and water condensation studies reveal the protective properties of coatings prepared by both materials as well as the superiority of Diamalloy 4276 based coatings. Corrosion was evaluated under a harsh 20% w/w H_2SO_4 environment. Rendering the coating superhydrophobic improves water condensation under the tested conditions of high (80%) relative humidity. [57]

The comprehensive edition of this publication can be found in Figure 5.

Key Engineering Materials
ISSN: 1662-9795, Vol. 963, pp 27-36
doi:10.4028/p-sth09H

Submitted: 2022-10-12
Revised: 2023-03-06
Accepted: 2023-04-19
Online: 2023-10-13

Development and Evaluation of Corrosion Resistance and Hydrophobic Properties of Thermal Sprayed Coatings over Carbon Steel

Paraskevi Nanou[1,2,a], John Konstantaras[1,2,b], Athanasios Zarkadoulas[1,2,c], Luca Montorsi[3,4,d], Hussam Jouhara[5,e], Vassilis Stathopoulos[1,f*]

[1]Laboratory of Chemistry and Materials Technology, Department of Agricultural Development, Agrofood and Management of Natural Resources, National and Kapodistrian University of Athens, Psachna Campus, 34400, Evia, Greece.

[2]University of Thessaly, Gaiopolis Campus – Ring Road of Larissa-Trikala, GR41500 Larissa Greece.

[3]Department of Sciences and Methods for Engineering – University of Modena and Reggio Emilia, via Amendola 2, 42122 Reggio Emilia, Italy.

[4]Centro Interdipartimentale EN&TECH, University of Modena and Reggio Emilia, Tecnopolo di Reggio Emilia, Piazzale Europa 1, 42124 Reggio Emilia, Italy.

[5]Heat Pipe and Thermal Management Research Group, College of Engineering, Design and Physical Sciences, Institute of Energy Futures, Brunel University London, UB8 3PH, UK

[a]nanoupar@uoa.gr, [b]yiannis.konstantaras@gmail.com, [c]azarkadoulas@uoa.gr, [d]luca.montorsi@unimore.it, [e]hussam.jouhara@brunel.ac.uk, [f]vasta@uoa.gr

Keywords: carbon steel, coating superhydrophobic, corrosion, superhydrophobic, thermal spraying

Abstract. Various industrial parts and equipment made of steel need to withstand demanding conditions. In order to increase performance and lifetime, surface processing and functional coatings can be applied. In this study we report on the evaluation of coated carbon steel with commercial corrosion-resistant powders Diamalloy 4276 and Woka 7502 by Oerlikon Metco, using thermal spraying. Further functionalization is performed by rendering thermal sprayed surfaces syperhydrophobic via gas phase deposition of trichloro-1H,1H,2H,2H-perfluorooctyl silane, (PFOTS). Electrochemical impedance spectroscopy, contact angle and water condensation studies reveal the protective properties of coatings prepared by both materials as well as the superiority of Diamalloy 4276 based coatings. Corrosion was evaluated under a harsh 20% w/w H_2SO_4 environment. Rendering the coating superhydrophobic improves water condensation under the tested conditions of high (80%) relative humidity.

Introduction

Metals and alloys are a predominant class of construction materials due to their versatility and the respective technological advancement in manufacturing and metal processing. Their main disadvantage is their corrosion susceptibility. Corrosion is destroying about 30% of the produced steel every year. According to ISO 8044:1986 the following definition is used: "corrosion is the physic-chemical interaction between a metal and its environment, which results in changes in the properties of the metal and which may often lead to impairment of the function of the metal, the environment, or the technical system of which these form a part" [1].

The harsh, corrosive environments existing in industrial processes where heat, water, and flue gases are at play put a strain on the overall efficiencies of procedures. Coatings or materials that have prolonged life under such harsh conditions, display versatility against various corroding agents such as SO_x [2,3] or high temperature oxidation [4,5] need to be used. A recent overview of the state of art of anticorrosion coatings mostly related to metals and alloys protection can be found in [1]. Such demanding conditions are to be met in the technologies developed and demonstrated under iWAYS project [6]. Technologies capable of recovering water and energy from challenging exhaust streams,

for productive use in three different energy and resource intensive industrial sectors: ceramic tile manufacturing, aluminium fluoride production and steel tubes manufacturing [6].

On the material selection, several points can be made; commercial metal alloys with extreme stability in corrosive environments exist such as Nimonic type alloys, Alloy 59, 400, C-276 etc. All having high nickel and chromium content. However, their cost is prohibiting for large scale applications, compared to stainless steel 304, 316, and carbon steel counterparts [7]. Development of coatings for low-cost Fe alloys that exhibit excellent corrosion resistance, similar to commercially available stainless-steel alloys or superalloys, has allowed to reduce cost for the fabrication of corrosion resistant technical equipment.

There are various methods developed, optimized and applied towards functional coatings [8]. One of the well-established methods is thermal spraying mainly applied in the energy and transportation sector towards protective coatings that facilitate higher combustion temperatures and thus improved engine efficiency, not only in power generation but also in aerospace and marine propulsion. Thus, metallic gas turbine engine components although made by refractory superalloys, are coated by thermal spraying with suitable Thermal Barrier Coatings (TBCs) protecting from the hot gas stream, high temperature corrosion, and subsequent failure. [9-11]. With this technique, semi-molten or molten material is sprayed with a high velocity on substrates. Thermal spraying can be applied with a plethora of coating materials, such as ceramic, metallic, or polymeric coatings, formed from precursors in powder form. The versatility of thermal spraying methods has had a large impact on wear resistance and corrosion protection applications [9-12]. Consequently, a great number of feed materials are market available, that according to their composition and chemical nature are capable of meeting versatile requirements of advanced applications in various technological sectors. Recent research has shown that post-treatment of thermal sprayed coatings using laser processing [13, 14] and/or surface modification with silane [14-16] can further enhance their properties. While laser post-treatment has been found to improve corrosion resistance, there are currently no reports on its effect on hydrophobicity [17]. By combining laser micro-texturing with silane modification, a superhydrophobic surface can be achieved [14]. Additionally, the spray parameters, such as particle velocity and temperature, play a critical role in determining the hydrophobicity of the coating. This is mainly due to the fact that the thermal spraying parameters affect the texture of the surface. Nano/microtexture along with the low surface energy are the controlling factors for the wetting properties of a surface. Specifically, high particle velocity is associated with superhydrophobic characteristics [13]. However, no reports on corrosion and hydrophobic bifunctional thermal sprayed coatings, where condensation occurs in dropwise manner has been reported recently. This is important due to the fact that hydrophobicity is not directly related to the efficiency of an engineering surfaces involved in applications where gas to liquid phase transitions occur through condensation. Such applications are water harvesting, air-cooling, power generation as well as waste heat recovery, etc.

Inspired by our previous reports in corrosion-resistant coatings [4,5], and having in mind the versatility of the thermal spraying technology along with the market availability of materials, in this work we report on the coating of carbon steel coupons with commercial Diamalloy 4276 and Woka 7502 powders by Oerlikon Metco [18,19]. These powders were selected by meeting the basic requirements of corrosion resistance in acidic conditions. Both were suitable to be applied by High Velocity Oxygen Fuel (HVOF) thermal spraying. While the Fe-alloy substrate coated and eventually protected is low-cost carbon steel known to readily corrode in the presence of humidity. HVOF was selected as it produces coatings of high density, which can lead to increased corrosion protection, since formation of cracks and crevices is minimised. [20] Eventually, protecting a low cost substrate such as carbon steel by thermal sprayed coatings is expected to prolonged material lifetime and overall enhance resource utilization. Such surfaces would be interesting to render hydrophobic, capable of delivering condensation in a dropwise manner, thus enhancing their applications potential.

By a post treatment, both the Diamalloy 4276 and Woka 7502 carbon steel coated surfaces were functionalized to produce super hydrophobic coatings. This unique property was achieved by gas phase deposition of trichloro-1H,1H,2H,2H-perfluorooctyl silane (PFOTS), in an effort to examine how superhydrophobicity acts synergistically with corrosion protection of coated, cheap steel alloys.

Figure 5. Comprehensive edition of "Development and Evaluation of Corrosion Resistance and Hydrophobic Properties of Thermal Sprayed Coatings over Carbon Steel"

Electrochemical impedance spectroscopy, contact angles, and water condensation studies were used to evaluate the protective properties of the developed coatings. Scanning electron microscopy was also used to evaluate the structural features of coating development of carbon steel substrates.

Experimental

Materials and Thermal Spray Coatings. Diamalloy 4276 is an alloy in powder form with high nickel and chromium content, resisting crevice and pitting corrosion under a variety of chemical attacks such as H_2SO_4 and chlorine environments. Woka 7502 is a carbide powder (chromium and tungsten) showing abrasion and cavitation resistance, with recommended applications in boilers, pumps and condensers, applications related to corrosive conditions. Thermal spray coatings of the above materials were applied over low-cost carbon steel. Both coating powders Diamalloy 4276 and Woka 7502 were purchased by Oerlikon Metco and used as received. The powders were thermal sprayed by a HVOF technique using an OERLIKON METCO 2700 DJM spray gun. In each case coatings of approx. 250 µm were applied on circular coupons of carbon steel with 2 in (5.08 cm) diameter, to produce specimens shown in Fig. 1. The resulting specimens were coated with Trichloro(1H,1H,2H,2H-perfluorooctyl)silane (PFOTS 97%, Aldrich) via a gas phase process, as described previously. [21]

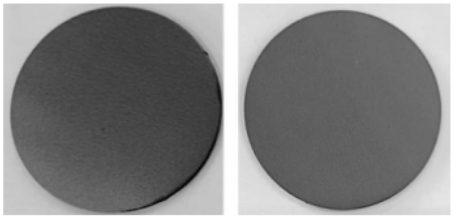

Figure 1. Optical images of Diamalloy 4276 (left) and Woka 7502 (right) coated carbon steel (CS) coupons (⌀ 2 in, 5.08 cm).

Surface characterization. Scanning electron microscope (SEM) images were obtained with a Phenom XL G2 instrument, from Thermo Fisher Scientific. The coatings were also evaluated using a stereoscope (Bel Photonics STMPro-T Led).

Corrosion Evaluation. In order to study the corrosion properties of the Diamalloy and Woka coatings the specimens were brought in contact with 20% w/w H_2SO_4 at 25 °C and their Electrochemical Impedance Spectrum (EIS) was periodically measured. EIS measurements were conducted prior to contact with the H_2SO_4 solution as well as after the 5th day of exposure. EIS was measured on both bare and coated samples using a three-electrode setup using an AMETEK VersaStat3 Potentiostat / Galvanostat Station [4]. Samples were used as Working Electrodes (WE), a platinum mesh used as the Counter Electrode (CE), and an Ag/AgCl electrode as the Reference Electrode (RE). All electrodes were immersed in a closed borosilicate beaker with 0.1 M H_2SO_4. The experimental setup is shown in Fig. 2.

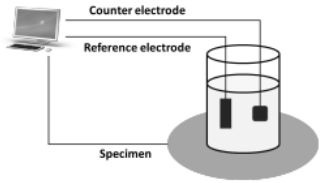

Figure 2. Electrochemical setup.

Contact Angles and Water Condensation. Condensation phenomena were recorded under 80% Relative Humidity (RH) at 30 °C in a custom-made water condensation chamber [22]. The coated specimen surface was maintained at 10 °C using a Peltier module. SL200 KS optical contact angle meter from Kino was used to measure contact angles applying Young-Laplace fitting method [23].

Results and Discussion

Surface characterization. Fig. 3 and Fig. 4 indicate that both Woka 7502 and Diamalloy 4276 coatings have uniform topography. They are dense and crack-free coatings and have low porosity and mostly uniformly melted regions. Spherical-shaped particles on the melted regions correspond to partially melted particles. These features are typical for high-velocity oxy-fuel (HVOF) deposition method, resulting in low porosity surfaces as well as a promising topography required for modifying their wetting behavior [20].

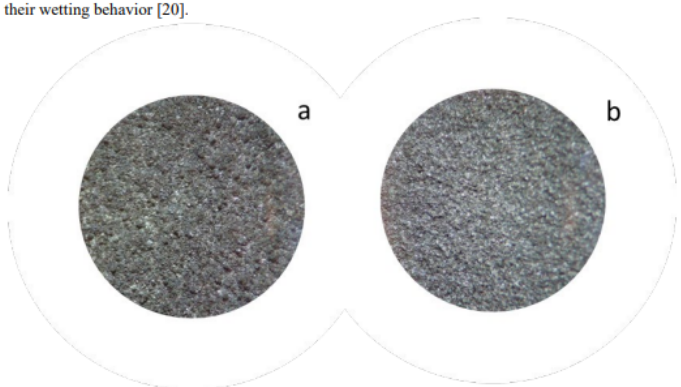

Figure 3. Stereoscope image 4.5x a)Diamalloy 4276 (left) and b)Woka 7502 (right) coated carbon steel (CS) coupons

Figure 5. (continued)

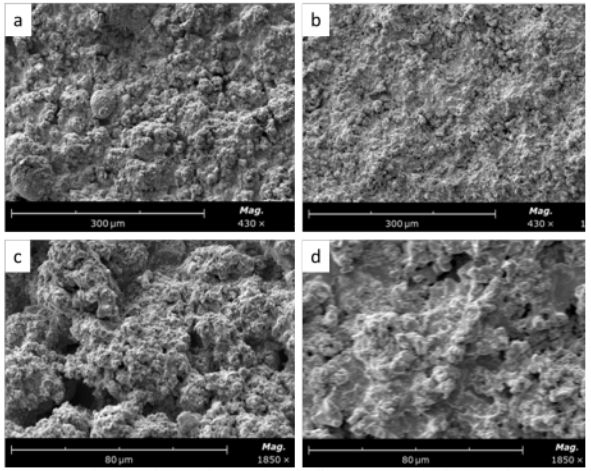

Figure 4. SEM images of thermal sprayed Diamalloy 4276 at magnification of (a) 430x and (c)1850x and Woka 7502 at magnification of 430x (b) and 1850x (d).

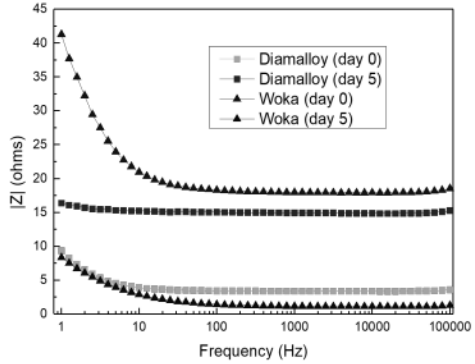

Figure 5. Bode plot for Diamalloy 4276 and Woka 7502 coated carbon steel coupons (day 0 and 5).

Electrochemical Corrosion Studies

The impedance modulus value at low frequencies is a commonly used indicator of the corrosion resistance performance of a coating. It reflects the corrosion process occurring at the interface between the coating and the corrosive electrolyte. Typically, a higher impedance modulus value at low frequency indicates better anti-corrosive performance [24].

Fig. 5 displays the Bode plots for Diamalloy and Woka coated carbon steel samples in 0.1 M sulfuric acid before and after their immersion in 20% w/w H_2SO_4. According to the Bode plots, the impedance modulus values of $|Z|_{1Hz}$ of Diamalloy coating at day 0 and 5 are 9.33 Ω and 16.34 Ω, respectively. This increase indicates that there was an improvement in the corrosion resistance of the sample [17]. After the first day, the coating behaves like a resistor, with its impedance being independent of frequency. This is reflected in the Bode magnitude plot, which is a horizontal straight line parallel to the frequency axis.

On the contrary, in Bode plots for Woka 7502 coating (Fig. 5), the impedance modulus values of $|Z|_{1Hz}$ of Woka 7502 coating at days 0 and 5 are 41.28 Ω and 8.32 Ω, respectively. The decrease of impedance modulus after immersion in the H_2SO_4 solution for 5 days indicates that the anti-corrosive properties of the coating gradually diminish.

These results are consistent with the current understanding of the relationship between impedance modulus value and anti-corrosive performance of coatings. Overall, the Diamalloy coating appears to have better corrosion resistance properties than the Woka 7502 coating based on the experimental data presented and the very harsh conditions applied. The increased chemical stability of Diamalloy 4276 compared to Woka 7502 is also evident macroscopically after 24 h of direct contact of each powder with 20% w/w H_2SO_4 solution (Fig. 6). The Diamalloy powder seems to be intact, in contrast to Woka powder, which reacts with the sulfuric acid. However, this should be considered only as an indicative result due to the fact that during thermal spray deposition the surface chemistry and properties of the feed powders are affected. Feed powders during the process and due to plasma may reach a semi-melted state. Thus, coatings are expected to exhibit modified features compared to the feed powder regarding on their chemical along with physical properties including chemical inertness. This is the reason why Woka coating appears of improved chemical inertness compared to the results of the pristine powder in contact to 20% w/w H_2SO_4 solution.

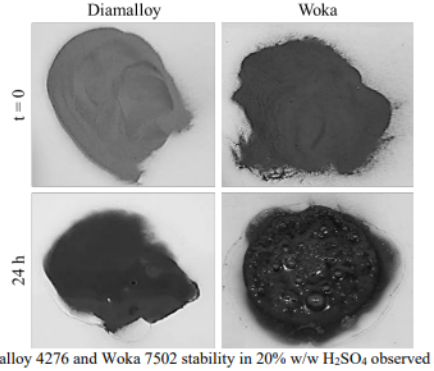

Figure 6. Diamalloy 4276 and Woka 7502 stability in 20% w/w H_2SO_4 observed after 24 h of contact.

Figure 5. (continued)

Contact Angles and Water Condensation

In order to render Diamalloy 4276 and Woka 7502-coated carbon steel coupons (super)hydrophobic and study condensation phenomena, a silane (trichloro-1H,1H,2H,2H-perfluorooctyl silane, PFOTS) was employed as a superhydrophobic coating using vacuum deposition, according to literature procedures [21,25-27].

Measurement of contact angles (CA) reveals that the surface of silane-coated coupons has become superhydrophobic (Fig. 7). CA of 145.6° ± 2.2° was found for Diamalloy and 151.3° ± 3.6° for Woka, PFOTS-coated-coupons, respectively. In terms of water roll-off angles, for the Diamalloy sample water roll-off angle measurement is impossible because the droplet remains pinned on the surface regardless of the testing angle, but on the Woka coupons a roll-off angle of 9° was measured.

The latter indicates different microstructure and/or topography in these two cases, because as A. Goswami et al. [28] allege, pinning is a result from the intermolecular forces between the solid and liquid, molecular level roughness, and surface topography including microporosity, other microscopic and chemical heterogeneities. PFOTS free Diamalloy and Woka coupons appear of super-hydrophilic nature under the HVOF conditions of deposition, as the water droplet readily infiltrated the coating during CA measurement.

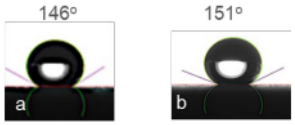

Figure 7. Water CAs measured for PFOTS-coated Diamalloy 4276 (left) and Woka 7502 (right) coupons.

To study further the wetting properties of the fabricated surfaces water condensation behavior was monitored. The study of condensation phenomena is important as condensation is a natural process applied in many industrial and engineering processes over interfaces made by engineering alloys. Understanding the mechanisms of condensation and the factors that affect it can lead to the development of more efficient surfaces, where the condensation mode will be dropwise. Dropwise condensation results in higher heat transfer, in comparison to filmwise condensation [28, 29]. DwC can be achieved by optimizing surface properties such as hydrophobicity and texture by using coatings demonstrated in this study, prepared by thermal spraying deposition and PFOTS.

Water condensation on both thermal sprayed and PFOTS-coated coupons reveals that in both cases, superhydrophobic, PFOTS-coated samples, perform better than untreated, thermal sprayed coated coupons (Fig. 8). Droplet nucleation initiates after 5 min of exposure in 80% RH for all samples, but condensation becomes more prominent after 10 min have elapsed; in this stage, the PFOTS-coated coupons exhibit dropwise condensation. Droplet coalescence proceeds with time, and after 60 min for PFOTS-coated coupons, condensation proceeds more readily. The absence of droplets on non-PFOTS-coated coupons after 60 min in the condensation chamber is attributed to their superhydrophilic nature and increased water infiltration (vide supra). This also points to the cause of trend observed in Bode plot (Fig. 5, Woka day 5), as the anti-corrosive properties of the alloy barrier levels off due to cracks and crevices of the coating.

In addition, it is interesting to point out that the PFOTS-coated coupons show stability of performance as they did not exhibit any decrease in CA values even after 1 h of water collection under condensation testing conditions.

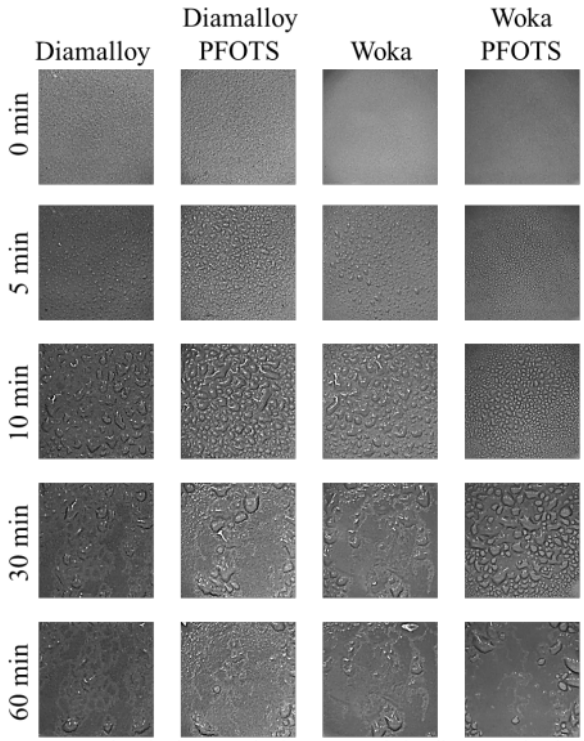

Figure 8. Water condensation for uncoated and PFOTS-coated Diamalloy 4276 and Woka 7502 carbon steel coupons.

Conclusions

The evaluation of two commercial materials against corrosion after their thermal spray deposition over carbon steel coupons has revealed increased stability for the case of Diamalloy 4276 compared to Woka 7502, under the demanding conditions applied in this study. HVOF of the metal powders under study provides good coverage of carbon steel coupons. Crack-free coatings are observed, with minimal porosity and mostly uniformly melted regions, with direct implications on corrosion resistance. Using Electrochemical Impedance Spectroscopy complementary with water condensation pattern observations revealed that in Woka 7502 cracks and crevices on the surface might contribute to the decreased stability of the coating. In terms of electrochemical corrosion resistance study, Diamalloy 4276 performs best in terms of corrosion resistance as evidenced by increasing impedance

Figure 5. (continued)

value after immersion in 20% w/w sulfuric acid. Woka 7502 exhibits better properties in terms of wetting and water condensation phenomena, with drop-wise condensation mode prevailing over film-wise condensation. However thermal spraying conditions may vary, affecting either deposition efficiency or coatings texture as mentioned previously [13-17]. The as reported promising results in relation to the versatility of thermal spraying deposition conditions as well methods, indicate that future studies may deliver interesting results. Thus, further study on such coatings for the control of their nano/microtextural features in relation to their corrosion protection as well as their wetting and water condensation properties is underway.

Acknowledgements

This research has been co-financed by the European Regional Development Fund of the European Union and Greek national funds through the Operational Program Competitiveness, Entrepreneurship and Innovation, under the call "Special Actions AQUACULTURE – INDUSTRIAL MATERIALS – OPEN INNOVATION IN CULTURE" (project code: T6YBP-00350). This work has received funding from the European Union's Horizon 2020 research and innovation programme under grant agreement No 958274

References

[1] V Kovalenko, V.Kotok, V.N. Stathopoulos, Smart coatings against corrosion, Encyclopedia of Smart Materials 1 (2022) 400-413.

[2] H. Jouhara, N. Khordehgah, S. Almahmou, B. Delpech, A. Chauhan, S. A.Tassou, Waste heat recovery technologies and applications, Therm. Sci. Eng. Prog. 6 (2018) 268-289.

[3] Z. Li, Y. Lu, R. S. Huang, J. Chang, X. Yu, R. Jiang, X. Yu, A. Roskilly, Applications and technological challenges for heat recovery, storage and utilisation with latent thermal energy storage, Applied Energy 283 (2021) 116277.

[4] V. Stathopoulos, V. Sadykov, S. Pavlova, Y. Bespalko, Y. Fedorova, L. Bobrova, A. Salanov, A. Ishchenko, V. Stoyanovsky, T. Larina, V. Ulianitsky, Z. Vinokurov, V. Kriventsov, Design of functionally graded multilayer thermal barrier coatings for gas turbine application, Surfaces & Coatings Technology 295 (2016) 20-28.

[5] N. Vourdas, E. Marathoniti, P.K. Pandis, Chr. Argirusis, G. Sourkouni, C. Legros, S. Mirza, V.N. Stathopoulos, Evaluation of $LaAlO_3$ as topcoat material for thermal barrier coatings, Transactions of Nonferrous Metals Society of China 28 (2018) 1582-1592.

[6] L. Montorsi, H. Jouhara, M. Venturelli, B Delpech, I. Celades Lopez, M-G. Asci, G. Bright, G. Jacomelli, D. Kroll, L, Zacares, M. Manfredini, D. Turesson, E. Rubion, V. Stathopoulos, R. Poskas, W. Gernjak, J. Santos, I. Marin, T. Stepisnik, D. Iatrou, A.Sayegh, "iWAYS - Recycling of heat, water and material across multiple sectors: ceramic, chemical and steel industry", (Proceedings of MSSM2022, 11-13 July 2022, Brunel University London-UK) Key Engineering materials, 2023 "under revision"

[7] Y. Kawahara, Application of high temperature corrosion-resistant materials and coatings under severe corrosive environment in waste-to-energy boilers, J. Therm. Spray Tech. 16 (2007) 202–213.

[8] V. Kotok, V.Kovalenko, V.N. Stathopoulos, Techniques for Coating Applications, Encyclopedia of Smart Materials 1 (2022) 243-257.

[9] N.P. Padture, M. Gell, E.H. Jordan, Thermal barrier coatings for gas-turbine engine applications, Science 296 (2002) 5566:280-284.

[10] D.R. Clarke, M. Oechsner, N.P. Padture, Thermal-barrier coatings for more efficient gas-turbine engines, MRS Bulletin 37 (2012) 10:891-898.

[11] H. Xu, H. Guo (2011) Thermal Barrier Coatings (Elsevier Science).

[12] P. K. Pandis, S. Papaioannou, V. Siaperas, A. Terzopoulos, V. N. Stathopoulos, Evaluation of Zn- and Fe- rich organic coatings for corrosion protection and condensation performance on waste heat recovery surfaces, Int. J. Thermofluids 3–4 (2020) 100025.

[13] S. M. Gateman, K. Page, I. Halimi, A. Nascimento, S. Savoie, R. Schultz, C. Moreau, I. P. Parkin, J. Mauzeroll, Corrosion of One-Step Superhydrophobic Stainless-Steel Thermal Spray Coatings, ACS Appl. Mater. Interfaces (2020), 12, 1, 1523–1532.

[14] V. Kumar, R. Verma, S. Kango, Micro-texturing of a WC–10Co–4Cr-Coated ASTM A479 Steel to Form a Super-Hydrophobic Surface, Transactions of the Indian Institute of Metals (2020) Volume 73, pages 1015–1026.

[15] Y.C. Li, W.W. Zhang, Y. Wang, X.Y. Zhang, L.L. Sun, Effect of spray powder particle size on the bionic hydrophobic structures and corrosion performance of Fe-based amorphous metallic coatings, Surface and Coatings Technology, Volume 437, 2022, 128377

[16] J. Liu, J. Wang, H. Memon, Y. Fu, T. Barman, K. Choi, X. Hou, Hydrophobic/icephobic coatings based on thermal sprayed metallic layers with subsequent surface functionalization, Surface and Coatings Technology (2019), Volume 357, 267-272.

[17] M. Buchtík, M. Hasoňová, P. Horník, M. Březina, L. Doskočil, J. Másilko, L. Mrňa, J. Filipenský, I. Kuběna, S. Fintová, J. Wasserbauer, P. Doležal, Influence of laser remelting on the microstructure and corrosion behavior of HVOF-sprayed Fe-based coatings on magnesium alloy, Materials Characterization (2022), Volume 194, 112343.

[18] https://mymetco.oerlikon.com/en-us/product/diamalloy4276

[19] https://mymetco.oerlikon.com/en-us/product/woka7502

[20] K. Palanisamy, S. Gangolu, J. Mangalam, Effects of HVOF spray parameters on porosity and hardness of 316L SS coated Mg AZ80 alloy, Surface and Coatings Technology (2022) 128898.

[21] A. Milionis, C. Noyes, E. Loth, I. S. Bayer, A. W. Lichtenberger, V. N. Stathopoulos, N. Vourdas, Water-Repellent Approaches for 3-D Printed Internal Passages, Materials and Manufacturing Processes 31 (2016) 1162-1170.

[22] P. Nanou, J. Konstantaras, A. Zarkadoulas, P. K. Pandis, N. Vourdas, V.N. Stathopoulos, Construction, evaluation and performance of a water condensation test unit, Proceedings of MSSM2022, 11-13 July 2022, Brunel University London-UK.

[23] V.Chalkia, N.Tachos, P.K. Pandis, A.Giannakas, Maria K. Koukou, M.Gr. Vrachopoulos, L.Coelho, A.Ladavos, V.N. Stathopoulos, Influence of organic phase change materials on the physical and mechanical properties of HDPE and PP polymers, RSC Advances 8 (2018) 27438-27447.

[24] B. Zhang, W. Xu, D. H. Xia, X. Fan, J. Duan, Y. Lu, Comparison Study of Self-Cleaning, Anti-Icing, and Durable Corrosion Resistance of Superhydrophobic and Lubricant-Infused Ultraslippery Surfaces, Langmuir 37 (2021) 11061-11071.

[25] M. Psarski, J. Marczak, G. Celichowski, G. B. Sobieraj, K. Gumowski, F. Zhou, W. Liu, Hydrophobization of epoxy nanocomposite surface with 1H,1H,2H,2H-perfluorooctyltrichlorosilane for superhydrophobic properties, Cent. Eur. J. Phys. 10 (2012) 1197-1201.

[26] N. Vourdas, C. Ranos, V.N. Stathopoulos, Reversible and dynamic transitions between sticky and slippery states on porous surfaces with ultra-low backpressure, RSC Advances 5 (2015) 33666-33673.

[27] N. Vourdas, K. Dalamagkidis and V. N. Stathopoulos, Active porous valves for plug actuation and plug flow manipulation in open channel fluidics, RSC Advances 5 (2015) 104594-104600.

[28] A. Goswami, S. C. Pillai, G. McGranaghan, Surface modifications to enhance dropwise condensation, Surfaces and Interfaces, Volume 25, 2021, 101143.

[29] N. Vourdas, H. Jouhara, S. A. Tassou, V. N. Stathopoulos, Design criteria for coatings in next generation condensing economizers, Energy Procedia (2019), Volume 161, 412-420

Figure 5. (continued)

2.9. Fabrication and Study of 3D Printed ABS-Carbon Composite Anodes for Single Chamber Microbial Fuel Cells, https://doi.org/10.4028/p-3QcQuv

Microbial Fuel Cells (MFCs) are electrochemical devices that exploit microbes for wastewater treatment with simultaneous power production. Concerning reactor design, electrode materials and operation modes, great achievements have been reported with an emphasis on developing anode materials to improve overall MFC performance. Anode materials (carbon cloth, carbon veil, carbon sponges) and their properties such as biocompatibility, electrical conductivity, surface area and efficient transport of waste play a very important role in power generation in MFCs.Despite their low cost, they present structural-based disadvantages eg. Fragility, and low conductivity issues. Additive manufacturing of Fused Deposition Modelling (FDM) due to its tailoring properties, has employed various polymer-based materials such as Polylactic Acid (PLA) and Acrylonitrile Butadiene Styrene (ABS) for manufacturing applications. In addition, carbon-based composites and hybrid materials eg. electrically conductive PLA and ABS have already been fabricated and are commercially available to exploit good electrical conductivity and structural rigidness. In this research, FDM was used to fabricate custom-sized electrodes made of a laboratory-produced electrically conductive ABS filament. A parametric study of conductivity and biocompatibility properties of these electrodes in correlation to 3D printer parameters was investigated and reported. Furthermore, treatment with a combination of thermal, mechanical, and chemical procedures was performed to improve the crucial parameters of anodes for MFCs. [66]

The comprehensive edition of this publication can be found in Figure 6.

Key Engineering Materials
ISSN: 1662-9795, Vol. 962, pp 113-120
doi:10.4028/p-3QcQuv

Submitted: 2022-10-13
Revised: 2023-04-13
Accepted: 2023-04-19
Online: 2023-10-12

Fabrication and Study of 3D Printed ABS-Carbon Composite Anodes for Single Chamber Microbial Fuel Cells

Pavlos K. Pandis[a*], Marina Georgala[b], Paraskevi Nanou[c], Vassilis N. Stathopoulos[d*]

Laboratory of Chemistry and Materials Technology, Department of Agricultural Development, Agrofood and Management of Natural Resources, National and Kapodistrian University of Athens, Psachna Campus, 34400, Evia, Greece

[a]ppandis@chemeng.ntua.gr, [b]marina.georgala@hotmail.com, [c]nanoupar@uoa.gr, [d]vasta@uoa.gr

Keywords: 3D printed, Microbial Fuel Cell, bioanode, biocompatibility, acclimation cycles

Abstract. Microbial Fuel Cells (MFCs) are electrochemical devices that exploit microbes for wastewater treatment with simultaneous power production. Concerning reactor design, electrode materials and operation modes, great achievements have been reported with an emphasis on developing anode materials to improve overall MFC performance. Anode materials (carbon cloth, carbon veil, carbon sponges) and their properties such as biocompatibility, electrical conductivity, surface area and efficient transport of waste play a very important role in power generation in MFCs. Despite their low cost, they present structural-based disadvantages eg. Fragility, and low conductivity issues. Additive manufacturing of Fused Deposition Modelling (FDM) due to its tailoring properties, has employed various polymer-based materials such as Polylactic Acid (PLA) and Acrylonitrile Butadiene Styrene (ABS) for manufacturing applications. In addition, carbon-based composites and hybrid materials eg. electrically conductive PLA and ABS have already been fabricated and are commercially available to exploit good electrical conductivity and structural rigidness. In this research, FDM was used to fabricate custom-sized electrodes made of a laboratory-produced electrically conductive ABS filament. A parametric study of conductivity and biocompatibility properties of these electrodes in correlation to 3D printer parameters was investigated and reported. Furthermore, treatment with a combination of thermal, mechanical, and chemical procedures was performed to improve the crucial parameters of anodes for MFCs.

1 Introduction

Microbial Fuel Cells (MFCs) are biochemical reactors that convert the chemical energy of waste substrates into power also lowering the levels of the waste's harmful characteristics, such as COD, BOD, conductivity, etc. These biochemical reactors consist of an anode and a cathode material [1-5], utilizing the organic load and microbial content of the waste to produce protons and electrons at the anode side which are transferred to the cathode side via electrolyte and external circuit, respectively as they react with oxygen to produce water. The electrode materials were investigated in order to improve the efficiency of the treatment of wastewater and energy generation. The electrode material should have excellent mechanical strength, chemical stability, biocompatibility, and electrical conductivity, among other characteristics. The conductive property of materials offers a high flow of electrons which is very important for MFC to perform well. The surface area of the electrode plays a significant role in microbial activity. Better performance was obtained by offering a higher surface area of the anode. Recently research advances in electrode materials, operations and designs have boosted MFCs electricity production and waste treatment efficiency [5-9]. In particular, anode materials selection and design are mainly focused on structures with biocompatibility, durability, and designs in favor of porosity and large surface area [2, 4, 10-13]. Microbial activity is easily affected by both the surface area and material composition of the anode [3, 14].
The Fused Deposition Modelling (FDM) of 3D printing is a versatile technique allowing rapid prototyping of tailored structures and is readily applied for polymer-based thermoplastic materials (PLA, ABS). Recently carbon modified PLA and ABS have become available exploiting good

electrical conductivity as well as good structural properties. Consequently, FDM may be considered for rapid prototyping of MFCs electrodes by such carbon modified functional polymers facilitating the design and scaling up manufacturing [15-20].
This study focused firstly on the production of an ABS-carbon polymer (ABSc) through a commercial extruder from Filastruder ltd. Various printing protocols were applied, via different nozzles and settings in a commercial 3D printer, in order to 3D print specimens of tailored features and examine their conductivity in correlation to the 3D printing parameters applied. Further, the specimens with the highest conductivity were subjected to thermal and chemical treatment in order to increase surface area, porosity and conductivity. The most promising samples were finally used as anodes in a single-chamber microbial fuel cell and acclimated in order to ensure and examine biocompatibility with anaerobic sludge from municipal waste and glucose as the substrate/synthetic waste.

2 Materials and Methods

2.1 Materials, Methods and Calculations

Acrylonitrile-Butadiene-Styrene (ABS) Pellets were purchased from 3DXTECH Inc and Activated Carbon (AC) (WS 380) from Calgon Carbon. ABS pellets were prior heated up to 80ºC for 1h to be initialized as the instructions for its use with extrusion were suggested. A mixture of 40%wt AC and 60%wt of ABS was prepared physically and then fed into a Filastruder v2.0 extruder (Figure 1).

Figure 1. Filastruder v2.0 extruder

The melting temperature of the extruder was set to 205ºC (before transition temperature) and the filament was produced at a diameter of 1.75mm. The as extruded filament was used as a feedstock for the 3D printing process in a Creality Ender 5 series Commercial 3D printer. Specimens of the following dimensions were printed: Length x Width x Height= 5 cm x 1cm x 1.5 cm. Printing parameters are depicted in Table 1.

Table 1. Specimens with different printing parameters

Code Name	Nozzle size (mm)	Initial Layer height (mm)	Layer Height (mm)	Infill (%)	Bed Temp (ºC)	Nozzle temp (ºC)	Top/Bottom Layers
ABSc_04_01	0.4	0.2	0.1	100	95	245	0.2
ABSc_04_02			0.2				0.4
ABSc_04_03			0.3				0.6
ABSc_06_01	0.6	0.3	0.1				0.2
ABSc_06_02			0.2				0.4
ABSc_06_03			0.3				0.6

The conductivity of the specimens was measured through Electrochemical impedance spectroscopy (EIS) with a VersaStat potensiostat/Galvanostat with two electrode configurations in specimens. The working electrode was attached to one side of the specimen and the counter and the reference electrode of the potentiostat were attached together on the other side. Conductivity (σ [S/m]) was then calculated via the conductivity equation:

$$\sigma = \frac{1}{Rs} \cdot \frac{L}{A} \quad (1)$$

where Rs is the ohmic value of the EIS spectrum of the specimen, L is the thickness and A is the area of the specimen.

Figure 6. Comprehensive edition of "Fabrication and Study of 3D Printed ABS-Carbon Composite Anodes for Single Chamber Microbial Fuel Cells"

Thermal treatment of the specimens was investigated with Thermogravimetric measurements in a Setaram STA unit subjecting 10mg of specimens under atmospheric air up to 800ºC with a heating rate of 2ºC/min [21] From the TGA diagrams appropriate temperature was selected prior to the transition point, and specimens with the best conductivity were treated at these temperatures for 30min [22].
Chemical treatment of specimens was conducted by immersion for 1 min into a 20%vol acetone - 80%vol deion-H_2O bath in a sonicated bath.
Both of the above treatments were applied in order to deliver two anodes: a. thermally (ABS-Th) and b. chemically (ABS-Ch) treated for testing them in a small-scale custom-made MFC as reported elsewhere [23].[X]
The COD, conductivity and pH value of the synthetic waste were measured after batch acclimation cycles of the cells. For this purpose, pH and conductivity were recorded using a digital pH meter and a conductivity meter with pH sensor (SEN0161) and conductivity sensor (DFR0300-H) modules purchased from DFRobot, China, while the COD measurements were performed according to standard methods [24].

2.2 Biocompatibility investigation of cells

Two different cells were equipped with the best thermally treated specimen and the best chemically treated respectively. The biocompatibility of the cells was investigated by monitoring the COD, pH and conductivity values achieved at the end of every acclimation cycle of the cells. Acclimation cycles were conducted with synthetic glucose substrate with the same cathodic electrodes as reported elsewhere [5, 23, 25, 26]. All operation cycles on the cells were tested in batch mode anaerobically and the final accepted values were acquired as the mean value of three different measurements. A total of 6 cycles using glucose as an organic substrate took place for the acclimatization of the cells and the duration of each acclimatization cycle was set at 10 days.
More specifically, during the acclimation period, 10% (v/v) of anaerobic sludge was obtained from the Athens (Greece) Wastewater Treatment Plant as the inoculum and a glucose-based synthetic effluent as the wastewater. In addition, 20 ml of a nutrient solution contained (per L): 5.29 g $NaH_2PO_4 \cdot 2H_2O$, 3.45 g $Na_2HPO_4 \cdot 2H_2O$, 0.16 g KCl, 5 g $NaHCO_3$ and 10 mL trace element solution was also used in order to culture the bacteriafrom sludge. The final synthetic waste was analyzed with the following characteristics: [COD=1000g/L, pH=6.61 and conductivity ~10.22 mS/cm^{-1}]. Cathode and anode were finally connected through a resistor of 100 kΩ prior of each acclimation cycle.

3 Results

3.1 Conductivity of 3D printed specimens

The produced filament from the extrusion process was used to 3D print specimens with specific parameters as mentioned in section 2.2. After obtaining the EIS spectra the calculated electrical conductivity of the samples is depicted in Table 2.

Table 2. Electrical conductivity of 3D printed samples with different parameters in comparison with other polymer composites in literature

Code Name	Conductivity (S/m)	Carbon source	Loading [%]	Reference
ABS	4.9×10^{-16}	n/a	n/a	[17]
ABSc_04_01	1.1×10^{-10}	Activated carbon	40	This work
ABSc_04_02	2.4×10^{-10}			This work
ABSc_04_03	3.2×10^{-10}			This work
ABSc_06_01	2.4×10^{-10}			This work
ABSc_06_02	2.7×10^{-10}			This work
ABSc_06_03	3.4×10^{-10}			This work
ABS/GNP	3.0×10^{-8}	Graphite nanoplates	6	[27]
ABS/CNT	2.3×10^{-4}	Carbon nanotubes	6	[17, 27]
ABS/Gr		Graphene	1	[28]
ABS/MWCNT	1.0×10^{-2}	Multi-wall carbon nanotubes	10	[29]

From Table 2, it seems that the addition of plain activated carbon (AC) may result in a significant increase in the electrical conductivity of the ABSc sample. The compared electrical conductivity values of the samples with other carbon sources such as graphite nanoplates, carbon nanotubes etc, shows that the samples of the present study can be considered promising due to the lower cost of the carbon source and the ease of preparation, despite the high loading reaching 40%wt.
For applications such as MFCs and with the prospect of further thermal and chemical treatment, ABSc specimens are viable candidates for anode substitutes of MFCs. Furthermore, it is obvious that the electrical conductivity of the samples printed with 0.6mm layer height is larger than those that have been printed with a layer height of 0.4mm. This is attributed to a lower boundary effect occurring due to larger layer height, and thicker and bulkier structures due to fewer layers for the same specimen dimensions. Electrical conductivity is totally related to bulk density and proportionally lowers with the increase of grain or layers boundaries.

3.2 TGA results and chemical treatments of specimens

ABSc_06_03 and ABSc_04_03 were subjected to TGA analysis. Their thermal behavior is depicted in Figure 4.

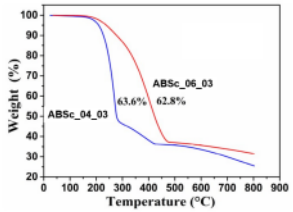

Figure 4. TGA analysis of samples ABSc_04_03 and ABSc_06_03

The decomposition of the two tested specimens begins at 201ºC and 206ºC respectively for ABSc_04_03 and ABSc_04_03 and evolves fast under ambient air. Therefore, the thermal treatment temperature is selected at 180ºC in order to avoid the deterioration of the matrixes. We have recently shown the effect of temperature on the features of 3D-printed structures [22]. Considering that

Figure 6. (continued)

structural features including layer boundaries can be modified with the processing temperature and the boundaries affect conductivity such a thermal treatment is expected to affect conductivity properties too. Thus ABSc_04_03-Th and ABSc_06_03-Th samples were prepared. The thermal decomposition of the sample ABSc_06_03 evolves faster due to smaller layer thickness, and thus less bulk total volume of the 3D printed sample. The value of conductivity of the two above samples has increased by the thermal treatment selected and the best choice is ABSc_06_03-Th, hence called ABSc-Th. Acetone is considered an ABS solvent. Thus, controlled exposure of ABS 3D printed specimens to acetone is expected to modify their surface features. Therefore, specimens ABSc_06_03 and ABSc_04_03 were subject to surface activation by immersion in acetone under simultaneous sonication. The acetone acts as a polar aprotic organic solvent that can generally dissolve a wide variety of polymers, especially after a long contact time. Thus, partial activation via limited and controlled partial dissolution on the layer-to-layer boundaries is expected to lead to better layer-to-layer affinity and also expected to minimize interlayer defects. As a result, the boundaries effect on conductivity may be positively affected causing improved conductivity properties too. The results of the above treatments, in terms of conductivity, are shown in Table 3.

Table 3. Conductivities of thermally and chemically treated specimens

Code Name	Conductivity (S/m)	Treatment
ABSc_04_03-Th	6.5×10^{-10}	Thermal
ABSc_06_03-Th	7.2×10^{-10}	Thermal
ABSc_04_03-Ch	5.8×10^{-10}	Chemical
ABSc_06_03-Ch	6.1×10^{-10}	Chemical

From the above values the best selections for their use in MFCs are ABSc_06_03-Th and ABSc_06_03-Ch (hence ABSc-Th and ABSc-Ch respectively). The proposed treatments have improved conductivity results of specimens maintaining the values of conductivity in the same order of magnitude though. Nevertheless, these increased conductivity values of 7.2×10^{-10} S/m and 6.1×10^{-10} S/m indicated that both the applied treatments had a remarkable effect.

3.3 Biocompatibility results of thermally and chemically treated specimens

The results of the biocompatibility tests as evaluated by the performance of the specimens over acclimation cycles are shown in Figure 6. In both sample cases, COD decreases very effectively, and stabilization provided evidence of microbial culturing onto the surfaces of the 3D-printed anodic electrodes. In the case of ABSc-Th the COD removal percentage is higher than the ABSc-Ch.

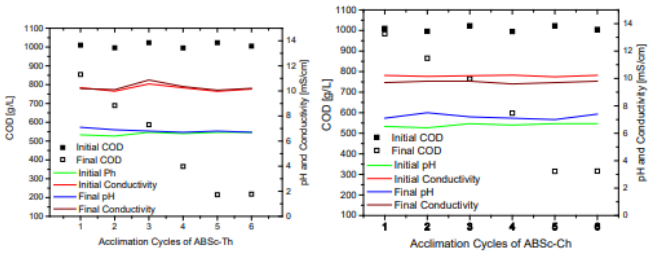

Figure 6. COD, pH and conductivity values of synthetic waste of ABSc-Th and ABSc-Ch anodes over MFC acclimation cycles

In the case of ABSc-Th from the first cycle a small drop of COD is observed at 851 g/L) and other values of pH and conductivity practically remained stable. A gradual drop of COD was further observed after each acclimation cycle providing a value of 215 g/L (78.5% COD removal) in the last two acclimation cycles. The fact that during the subsequent cycles the values of pH and conductivity remained at the values of 6.7 and 10.35 mS/cm respectively, indicated the proper condition of acclimation onto the anode without changing the conductivity conditions of the synthetic waste.
I the case of ABS-Ch a gradual drop of COD was also observed with lower efficiency in comparison with ABSc-Th. More specifically, from the first acclimation cycle there was practically minimum COD removal, maintaining a value for COD at 984 g/L whilst a gradual drop of the values of COD followed to reach a COD removal of 68% (COD=315 g/L) in the last two cycles. Although the values of pH were not affected during these cycles maintaining the value of 6.8, the values of conductivity were dropped from the first cycle at 9.8 mS/cm indicating a barrier in the acclimation process.
Nevertheless, both MFC configurations provided a total COD removal over 65% which indicated a favoured acclimation of bacteria from the sludge onto the 3D printed surfaces.

4 Conclusions

In this work, ABS conductive filament containing 40%wt activated carbon was successfully prepared and used for 3D printing. This production was achieved through a commercial extruder with the direct mixing of activated carbon with ABS pellets. The parametric study of conductivity correlation with 3D printed parameters verified that the larger the nozzle size of the 3D printer the higher conductivity of the produced ABS conductive filament. The measured conductivity of the prepared samples was lower than other ABS conductive filament with CNTs, MWCNT, Graphene etc reported in the literature indicating the need for further investigation on aspects such as AC loading, dispersion and ABS –AC interface modifications in order to enhance the electrical properties within the ABS matrix. Thermal and chemical treatments of produced 3D specimens led to an increase in the electrical conductivity of the samples indicating the crucial role of the boundary effect. The results of biocompatibility experiments verified the initial concept about their suitability as anodes in single-chamber MFCs. Better results were recorded for the thermally treated 3D anodes that proved to preferably favor microbial activity in comparison to the chemically treated samples. These results open a new way of utilizing FDM technology in shaping and treating custom-made anodes in MFCs leading to the concept of modular structures in MFC technology.

References

[1] P. Zhang, C. Yang, Y. Xu, H. Li, W. Shi, X. Xie, M. Lu, L. Huang, W. Huang, Accelerating the startup of microbial fuel cells by facile microbial acclimation, Bioresource Technology Reports, 8 (2019) 100347.

[2] K. Sakai, S. Iwamura, R. Sumida, I. Ogino, S.R. Mukai, Carbon Paper with a High Surface Area Prepared from Carbon Nanofibers Obtained through the Liquid Pulse Injection Technique, ACS Omega, 3 (2018) 691-697.

[3] S. Li, C. Cheng, A. Thomas, Carbon-Based Microbial-Fuel-Cell Electrodes: From Conductive Supports to Active Catalysts, Advanced Materials, 29 (2017) 1602547.

[4] A.A. Yaqoob;, M.N.M. Ibrahim;, M.Rafatullah;, Y.S. Chua;, A.Ahmad;, K. Umar, Recent Advances in Anodes for Microbial Fuel Cells: An Overview, Materials (Basel), 13 (2020).

[5] A. Tremouli, T. Kamperidis, P.K. Pandis, Ch. Argirusis, G. Lyberatos, Exploitation of digestate from thermophilic and mesophilic anaerobic digesters fed with fermentable food waste using the MFC technology, Waste and Biomass Valorization, (2021).

[6] P. Liang, J. Wei, M. Li, X. Huang, Scaling up a novel denitrifying microbial fuel cell with an oxic-anoxic two stage biocathode, Frontiers of Environmental Science & Engineering, 7 (2013) 913-919.

Figure 6. (continued)

[7] B.E. Logan, M.J. Wallack, K.-Y. Kim, W. He, Y. Feng, P.E. Saikaly, Assessment of Microbial Fuel Cell Configurations and Power Densities, Environmental Science & Technology Letters, 2 (2015) 206-214.

[8] V. Lanas, Y. Ahn, B.E. Logan, Effects of carbon brush anode size and loading on microbial fuel cell performance in batch and continuous mode, Journal of Power Sources, 247 (2014) 228-234.

[9] J. Wei, P. Liang, X. Huang, Recent progress in electrodes for microbial fuel cells, Bioresource Technology, 102 (2011) 9335-9344.

[10] G.G. kumar, V.G.S. Sarathi, K.S. Nahm, Recent advances and challenges in the anode architecture and their modifications for the applications of microbial fuel cells, Biosensors and Bioelectronics, 43 (2013) 461-475.

[11] Y. Hindatu, M.S.M. Annuar, A.M. Gumel, Mini-review: Anode modification for improved performance of microbial fuel cell, Renewable and Sustainable Energy Reviews, 73 (2017) 236-248.

[12] D. Sauerteig, N. Hanselmann, A. Arzberger, H. Reinshagen, S. Ivanov, A. Bund, Electrochemical-mechanical coupled modeling and parameterization of swelling and ionic transport in lithium-ion batteries, Journal of Power Sources, 378 (2018) 235-247.

[13] M.I. Din, M. Iqbal, Z. Hussain, R. Khalid, Bioelectricity generation from waste potatoes using single chambered microbial fuel cell, Energy Sources, Part A: Recovery, Utilization, and Environmental Effects, (2020) 1-11.

[14] A.A. Yaqoob, M.N.M. Ibrahim, S. Rodríguez-Couto, Development and modification of materials to build cost-effective anodes for microbial fuel cells (MFCs): An overview, Biochemical Engineering Journal, 164 (2020) 107779.

[15] P.J. Brigandi, J.M. Cogen, R.A. Pearson, Electrically conductive multiphase polymer blend carbon-based composites, Polymer Engineering & Science, 54 (2014) 1-16.

[16] B.G. Compton, J.A. Lewis, 3D-Printing of Lightweight Cellular Composites, Advanced Materials, 26 (2014) 5930-5935.

[17] S. Dul, B.J.A. Gutierrez, A. Pegoretti, J. Alvarez-Quintana, L. Fambri, 3D printing of ABS Nanocomposites. Comparison of processing and effects of multi-wall and single-wall carbon nanotubes on thermal, mechanical and electrical properties, Journal of Materials Science & Technology, 121 (2022) 52-66.

[18] J. Ouyang, Recent Advances of Intrinsically Conductive Polymers, Acta Physico-Chimica Sinica, 34 (2018) 1211-1220.

[19] B. Podsiadły, P. Matuszewski, A. Skalski, M. Słoma, Carbon Nanotube-Based Composite Filaments for 3D Printing of Structural and Conductive Elements, Applied Sciences, 11 (2021) 1272.

[20] Sachin C. Kulkarni, Jitendra Singh, D.K. Shinde, Mechanical and Electrical Properties of Carbon Nanotubes Based Acrylonitrile Butadiene Styrene Nanocomposite Fabricated Using Fused Deposition Method, in: SAMPE 2019, CHARLOTTE, NC 2019.

[21] P.K. Pandis, S. Papaioannou, M.K. Koukou, M.G. Vrachopoulos, V.N. Stathopoulos, Differential scanning calorimetry based evaluation of 3D printed PLA for phase change materials encapsulation or as container material of heat storage tanks, in: 2nd International Conference on Sustainable Energy and Resource Use in Food Chains, ICSEF 2018, Paphos, Cyprus, 2018.

[22] O. Luzanin, D. Movrin, V. Stathopoulos, P. Pandis, T. Radusin, V. Guduric, Impact of processing parameters on tensile strength, in-process crystallinity and mesostructure in FDM-fabricated PLA specimens, Rapid Prototyping Journal, 25 (2019) 1398-1410.

[23] P.K. Pandis, T. Kamperidis, K. Bariamis, I. Vlachos, C. Argirusis, V.N. Stathopoulos, G. Lyberatos, A. Tremouli, Comparative Study of Different Production Methods of Activated Carbon Cathodic Electrodes in Single Chamber MFC Treating Municipal Landfill Leachate, Applied Sciences, 12 (2022) 2991.

[24] T. Kamperidis, P.K. Pandis, C. Argirusis, G. Lyberatos, A. Tremouli, Effect of Food Waste Condensate Concentration on the Performance of Microbial Fuel Cells with Different Cathode Assemblies, Sustainability, 14 (2022) 2625.

[25] A. Tremouli, P.K. Pandis, T. Kamperidis, V.N. Stathopoulos, C. Argirusis, G. Lyberatos, Performance assessment of a four-air cathode membraneless microbial fuel cell stack for wastewater treatment and energy extraction, E3S Web of Conferences, 116 (2019) 00093.

[26] A. Tremouli, P.K. Pandis, I. Karydogiannis, V.N. Stathopoulos, C. Argirusis, G. Lyberatos, Operation and Electro(chemical) characterization of a microbial fuel cell stack fed with fermentable household waste extract, Global NEST Journal, 21 (2019) 253-257.

[27] S. Dul, L. Fambri, A. Pegoretti, Filaments Production and Fused Deposition Modelling of ABS/Carbon Nanotubes Composites, Nanomaterials (Basel), 8 (2018).

[28] X. Liu, Q. Zou, T. Wang, L. Zhang, Electrically Conductive Graphene-Based Biodegradable Polymer Composite Films with High Thermal Stability and Flexibility, Nano, 13 (2018) 1850033.

[29] H.K. Sezer, O. Eren, FDM 3D printing of MWCNT re-inforced ABS nano-composite parts with enhanced mechanical and electrical properties, Journal of Manufacturing Processes, 37 (2019) 339-347.

Figure 6. (continued)

3. Scientific conferences

The laboratory has actively participated in 39 international conferences the last 10 years, where researchers have presented their latest findings and engaged in scholarly discourse. These conferences serve as invaluable platforms for knowledge dissemination, facilitating exchanges of ideas and fostering collaborations with peers from around the world. Specifically, some of the conferences that LCMT team participated are Applied Nanotechnology and Nanoscience International Conference - ANNIC 2015, 12th European Congress on Catalysis – EuropaCat-XII, European Congress and Exhibition on Advanced Materials and Processes-EUROMAT 2015, International Conference On Applied Mineralogy & Advanced Materials, 5th Nano Today Conference, 2nd International Conference on Sustainable Energy and Resource Use in Food Chains, ICSEF 2018, 12th International Conference on Sustainable Energy & Environmental Protection "SEEP 2019", 9th International Workshop on Advances in Cleaner Production Towards Sustainable Energy-Water-Food Nexus: The Contribution of Cleaner Production, 17th International Conference on Environmental Science and Technology, and 8th International Conference on Material Science & Smart Materials “MSSM 2022”.

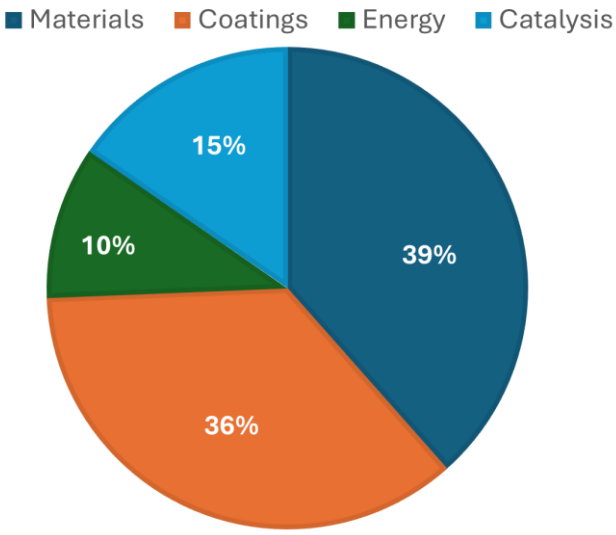

Figure 7. LCMT conference contributions fields 2014-2024

Catalysis remains a prominent focus of LCMT's conference presentations, comprising 15% of the laboratory's contributions. LCMT researchers have shared their insights into catalytic mechanisms, novel catalyst design, and catalytic process optimization at conferences spanning the globe. These presentations have facilitated the exchange of ideas and catalyzed collaborations with researchers from academia, and industry, ultimately advancing the field of catalysis and its applications in various sectors.

Materials science continues to be a cornerstone of LCMT's conference participation, accounting for 39% of the laboratory's presentations. LCMT researchers have

showcased their expertise in materials synthesis, characterization, and application at conferences covering a wide range of topics, such as nanomaterials and polymers and composites. Through their conference presentations, LCMT researchers have contributed to the collective knowledge base of materials science, while also forging connections with peers and collaborators from around the world.

Energy-related research has emerged as a growing area of interest for LCMT, representing 10% of the laboratory's conference presentations. LCMT researchers have shared their findings on topics such as energy storage, renewable energy, and sustainable fuel production at conferences focused on energy technologies and environmental sustainability. These presentations have stimulated discussions on pressing energy challenges and potential solutions, paving the way for collaborative efforts aimed at addressing global energy needs.

Coatings research has garnered significant attention at LCMT's conference presentations, comprising 36% of the laboratory's contributions. LCMT researchers have shared their expertise in surface chemistry, thin film deposition, and coating technologies at conferences dedicated to coatings and surface engineering. These presentations have highlighted the role of coatings in enhancing the performance, durability, and functionality of diverse materials and devices, while also fostering collaborations with industry partners seeking innovative coating solutions.

The 2023 LCMT scientific team made remarkable strides in showcasing their research, with a total of 10 contributions presented at prestigious conferences. The team's dedication and expertise were evident as they presented eight works at the EMANATE CONFERENCE 2023, a significant platform for exchanging ideas and advancements in various fields. At EMANATE CONFERENCE 2023, the team's presentations covered a diverse range of topics, spanning from fundamental research to applied technologies, reflecting the multidisciplinary nature of their work.

Namely the influence of urban fires on the concentration of mobile forms of elements of concern and heavy metals in surface and in different soil depths were investigated. Sampling of soils of pyrogenic origin was carried out in 2022 by at least 800 different ground sampling points. All points selected according to operating standards in the territory of Mati and Kineta (Attica, Greece) that suffered from wildfires in July of 2018. The heavy metals content of the soil samples was identified after Aqua Regia extraction utilizing Inductively coupled plasma-mass spectrometry (ICP-MS) as analytical method. Certified Reference Materials (CRM) were used for the method development. The results were evaluated using the Dutch List, a collection of values and regulations related with the contaminated soils[67].

The need for suitable training and methods and material for the introduction of green special processes in aerospace industry was discussed during EMANATE by members of LCMT in collaboration with the Hellenic Airspace Industry. Special processes (Welding, Surface Engineering & Chemical Processing, Electronics manufacturing, Composites, Elastomer Seals, Heat Treatment, Thermal Spraying, Materials Testing & Inspection, Nonconventional Machining, Non-destructive Testing etc) in materials for specific applications such as aircraft and aircraft engines Maintenance Repair and Overhaul (MRO) require specific and advanced skills, equipment, and detailed procedures to ensure the quality and safety of the maintenance work [68].

The manganese based mixed oxides were discussed for their properties as well as for their structure and composition effect on their catalytic performance in typical redox reactions. Such structural features were introduced by the synthesis method applied and both composition and structural characteristics can be used to control the catalytic performance. By the synthesis method rare earths, transition metals and or alkaline earths can be introduced towards mixed systems as well as perovskite structure formation [69]. Similar perovskites type oxides were studied for solid oxide electrolytic cells (SOECs) cathodes. The aim was to develop A-site deficient perovskite materials of exceptional redox stability and tailored ionic-electronic conducting properties for efficient syngas production in reversible solid oxide electrolysis/fuel cells, utilizing the reaction $CO_2 + H_2O \rightleftarrows CO + H_2 + O_2$. Candidate cathode materials were prepared and reported, utilizing the LSCM (La, Sr, Cr, X) formulation of perovskite oxide material, with the general formula $La_{0.75}Sr_{0.25}Cr_{0.5}X_{0.5}O_{3-\delta}$ (X=Mn, Fe). Several B-site doping strategies in A-site deficient perovskites have also been employed, with the ultimate goal of studying the formation of mono- or multi-metallic nanoparticles obtained after exsolution [70].

The Microbial Fuel Cells (MFCs) that gain popularity as cutting-edge biochemical reactors that consume waste substrates in order for the electrogenic bacteria and/or enzyme cultures to produce electricity and, simultaneously, to lower environmentally hazardous values of wastes were in LCMT research focus. Results of this research were reported, as a single chamber microbial fuel cell was operated with commercial steel sponges as anode electrodes, and ceramic electrodes as a cathode, whilst the use of Escherichia coli (E. coli) bacteria was evaluated as the bacteria for treating tannery waste. Stainless steel electrodes outperformed carbon felt in terms of power generation and COD tannery treatment. A COD decrease of almost 80% was achieved with stainless steel followed by an increased power output of 50% in comparison with carbon-felt electrode [71].

The group in collaboration with other research groups and an enterprise through funded projects reported on the development and study of properties of super-hydrophobic surface morphology on sandblasted stainless steel 304 samples. The findings of this study were promising and further studies are underway [72]. In the same subject the group reported the superior durability, superhydrophobicity, and corrosion protection of

functional coatings over 304 stainless steel [73] as well as on three types functional coatings applied by thermal spraying to provide protection against corrosion and fatigue, resulting in prolonged lifespan, reduced material waste, and improved resource economy. In this study, the effectiveness of three types of functional coatings applied via thermal spraying to carbon steel was evaluated. Electrochemical measurements, and contact angle studies were then conducted to assess the coatings' effectiveness under harsh corrosive conditions with sulfates present [74]. Functional coatings for flat-type solar panels were also reported as applied using physical spraying method and tested. The precursors were water based VOC free [75].

Their contributions not only highlighted their innovative approaches but also fostered collaboration and discussion among peers in the scientific community. Additionally, the team showcased two works at the 9th International Conference on Material Science & Smart Materials “MSSM 2023”. This conference provided a focused platform for sharing insights and developments in material science and smart materials, areas crucial for advancements in numerous industries including electronics, healthcare, and energy.

The team's participation in these conferences underscores their commitment to pushing the boundaries of knowledge and driving progress in their respective fields. By sharing their research findings and engaging with fellow experts, they contribute significantly to the collective effort of advancing science and technology for the betterment of society.

4. Conclusions and Remarks

The Laboratory of Chemistry and Materials Technology (LCMT) has demonstrated exceptional prowess and dedication in scientific research throughout the year 2023. Through a multifaceted approach encompassing both publications and conference contributions, LCMT has made significant strides in advancing knowledge and innovation in the fields of chemistry and materials technology.

LCMT's scientific publications in 2023 span a diverse range of research areas, including catalysis, materials science, energy research, and coatings. These publications not only highlight the laboratory's depth of expertise but also its commitment to addressing pressing societal challenges through interdisciplinary collaboration and innovative solutions.

Furthermore, LCMT's active participation in international conferences underscores its commitment to scholarly discourse and knowledge dissemination. By presenting their latest findings and engaging with peers from around the world, LCMT researchers have fostered collaboration and facilitated the exchange of ideas, ultimately contributing to the collective advancement of science and technology.

In summary, LCMT's achievements in 2023 underscore its position as a leader in scientific research, driving innovation and shaping the future of chemistry and materials technology. Through its continued dedication to excellence and interdisciplinary collaboration, LCMT is poised to make even greater contributions to scientific knowledge and societal progress in the years to come.

References

[1] G. Varvoutis, A. Lampropoulos, P. Oikonomou, C.-D. Andreouli, V. Stathopoulos, M. Lykaki, G.E. Marnellos, M. Konsolakis, Fabrication of highly active and stable Ni/CeO2-nanorods wash-coated on ceramic NZP structured catalysts for scaled-up CO2 methanation, Journal of CO2 Utilization 70 (2023) 102425. https://doi.org/10.1016/j.jcou.2023.102425.

[2] A. Tremouli, P.K. Pandis, T. Kamperidis, C. Argirusis, V.N. Stathopoulos, G. Lyberatos, Performance Comparison of Different Cathode Strategies on Air-Cathode Microbial Fuel Cells: Coal Fly Ash as a Cathode Catalyst, Water 15 (2023). https://doi.org/10.3390/w15050862.

[3] M. Konsolakis, V.N. Stathopoulos, Rational Design of Non-Precious Metal Oxide Catalysts by Means of Advanced Synthetic and Promotional Routes, Catalysts 11 (2021). https://doi.org/10.3390/catal11080895.

[4] C.B. Anucha, E. Bacaksiz, V.N. Stathopoulos, P.K. Pandis, C. Argirusis, C.-D. Andreouli, Z. Tatoudi, I. Altin, Molybdenum Modified Sol–Gel Synthesized TiO2 for the Photocatalytic Degradation of Carbamazepine under UV Irradiation, Processes 10 (2022). https://doi.org/10.3390/pr10061113.

[5] C.B. Anucha, E. Bacaksiz, V.N. Stathopoulos, P.K. Pandis, C. Argirusis, C.-D. Andreouli, Z. Tatoudi, I. Altin, Preparation and Characterization of Supported Molybdenum Doped TiO2 on α-Al2O3 Ceramic Substrate for the Photocatalytic Degradation of Ibuprofen (IBU) under UV Irradiation, Catalysts 12 (2022). https://doi.org/10.3390/catal12050562.

[6] C.B. Anucha, I. Altin, E. Bacaksiz, V.N. Stathopoulos, Titanium dioxide (TiO_2)-based photocatalyst materials activity enhancement for contaminants of emerging concern (CECs) degradation: In the light of modification strategies, Chemical Engineering Journal Advances 10 (2022) 100262. https://doi.org/10.1016/j.ceja.2022.100262.

[7] M. Konsolakis, V. Stathopoulos, Preface on recent advances on surface and interface functionalization in Nano-Catalysis (SUR-INTER-CAT), Applied Surface Science Advances 5 (2021) 100093. https://doi.org/10.1016/j.apsadv.2021.100093.

[8] C.B. Anucha, Ii. Altin, E. Bacaksiz, V.N. Stathopoulos, I. Polat, A. Yasar, Ö.F. Yüksel, Silver Doped Zinc Stannate (Ag-ZnSnO3) for the Photocatalytic Degradation of Caffeine under UV Irradiation, Water 13 (2021). https://doi.org/10.3390/w13091290.

[9] Z. Savva, K.C. Petallidou, C.M. Damaskinos, G.G. Olympiou, V.N. Stathopoulos, A.M. Efstathiou, H2-SCR of NOx on low-SSA CeO2-supported Pd: The effect of Pd particle size, Applied Catalysis A: General 615 (2021) 118062. https://doi.org/10.1016/j.apcata.2021.118062.

[10] V. Cortés Corberán, V. Rives, V. Stathopoulos, Chapter 7 - Recent Applications of Nanometal Oxide Catalysts in Oxidation Reactions, in: V.A. Sadykov (Ed.), Advanced

Nanomaterials for Catalysis and Energy, Elsevier, 2019: pp. 227–293. https://doi.org/10.1016/B978-0-12-814807-5.00007-3.
[11] P.K. Pandis, D.E. Perros, V.N. Stathopoulos, Doped apatite-type lanthanum silicates in CO oxidation reaction, Catalysis Communications 114 (2018) 98–103. https://doi.org/10.1016/j.catcom.2018.06.017.
[12] M.A. Goula, N.D. Charisiou, P.K. Pandis, V.N. Stathopoulos, A Ni/apatite-type lanthanum silicate supported catalyst in glycerol steam reforming reaction, RSC Adv. 6 (2016) 78954–78958. https://doi.org/10.1039/C6RA10437A.
[13] C.B. Anucha, Ii. Altin, D. Fabbri, I. Degirmencioglu, P. Calza, G. Magnacca, V.N. Stathopoulos, E. Bacaksiz, Synthesis and Characterization of B/NaF and Silicon Phthalocyanine-Modified TiO2 and an Evaluation of Their Photocatalytic Removal of Carbamazepine, Separations 7 (2020). https://doi.org/10.3390/separations7040071.
[14] C.B. Anucha, I. Altin, E. Bacaksız, T. Kucukomeroglu, M.H. Belay, V.N. Stathopoulos, Enhanced Photocatalytic Activity of CuWO4 Doped TiO2 Photocatalyst Towards Carbamazepine Removal under UV Irradiation, Separations 8 (2021). https://doi.org/10.3390/separations8030025.
[15] C. BethelAnucha, Ii. Altin, E. Bacaksiz, I. Degirmencioglu, T. Kucukomeroglu, S. Yılmaz, V.N. Stathopoulos, Immobilized TiO2/ZnO Sensitized Copper (II) Phthalocyanine Heterostructure for the Degradation of Ibuprofen under UV Irradiation, Separations 8 (2021). https://doi.org/10.3390/separations8030024.
[16] S. Stefa, M. Lykaki, V. Binas, P.K. Pandis, V.N. Stathopoulos, M. Konsolakis, Hydrothermal Synthesis of ZnO–doped Ceria Nanorods: Effect of ZnO Content on the Redox Properties and the CO Oxidation Performance, Applied Sciences 10 (2020). https://doi.org/10.3390/app10217605.
[17] S. Stefa, M. Lykaki, D. Fragkoulis, V. Binas, P.K. Pandis, V.N. Stathopoulos, M. Konsolakis, Effect of the Preparation Method on the Physicochemical Properties and the CO Oxidation Performance of Nanostructured CeO2/TiO2 Oxides, Processes 8 (2020). https://doi.org/10.3390/pr8070847.
[18] M. Lykaki, S. Stefa, S.A.C. Carabineiro, P.K. Pandis, V.N. Stathopoulos, M. Konsolakis, Facet-Dependent Reactivity of Fe2O3/CeO2 Nanocomposites: Effect of Ceria Morphology on CO Oxidation, Catalysts 9 (2019). https://doi.org/10.3390/catal9040371.
[19] C.M. Damaskinos, M.A. Vasiliades, V.N. Stathopoulos, A.M. Efstathiou, The Effect of CeO2 Preparation Method on the Carbon Pathways in the Dry Reforming of Methane on Ni/CeO2 Studied by Transient Techniques, Catalysts 9 (2019). https://doi.org/10.3390/catal9070621.
[20] K.M. Sideris, D. Fragoulis, V.N. Stathopoulos, P. Sinioros, Multi-Layer Ceramic Capacitors in Lighting Equipment: Presence and Characterisation of Rare Earth Elements and Precious Metals, Recycling 8 (2023). https://doi.org/10.3390/recycling8060097.
[21] P.K. Pandis, T. Kamperidis, K. Bariamis, I. Vlachos, C. Argirusis, V.N. Stathopoulos, G. Lyberatos, A. Tremouli, Comparative Study of Different Production Methods of Activated Carbon Cathodic Electrodes in Single Chamber MFC Treating Municipal Landfill Leachate, Applied Sciences 12 (2022). https://doi.org/10.3390/app12062991.
[22] Y. Bespalko, T. Kuznetsova, T. Kriger, Y. Chesalov, O. Lapina, A. Ishchenko, T. Larina, V. Sadykov, V. Stathopoulos, La2Zr2O7/LaAlO3 composite prepared by mixing

precipitated precursors: Evolution of its structure under sintering, Materials Chemistry and Physics 251 (2020) 123093. https://doi.org/10.1016/j.matchemphys.2020.123093.
[23] C. Jiménez-Holgado, C. Chrimatopoulos, V. Stathopoulos, V. Sakkas, Investigating the Utility of Fabric Phase Sorptive Extraction and HPLC-UV-Vis/DAD to Determine Antidepressant Drugs in Environmental Aqueous Samples, Separations 7 (2020). https://doi.org/10.3390/separations7030039.
[24] A. Inayat, Z. Said, O. Alsaidi, R. Al-Zaidi, S. Ullah, V. Stathopoulos, Review of Recent Progress in Wastewater Treatment Using Carbon Nanotubes, Current Analytical Chemistry 17 (2021). https://doi.org/10.2174/1573411016999200709134020.
[25] O. Luzanin, D. Movrin, V. Stathopoulos, P. Pandis, T. Radusin, V. Tiodorovic Neé Guduric, Impact of processing parameters on tensile strength, in-process crystallinity and mesostructure in FDM-fabricated PLA specimens, Rapid Prototyping Journal ahead-of-print (2019). https://doi.org/10.1108/RPJ-12-2018-0316.
[26] N. Vourdas, G. Pashos, E. Rizos, G. Kokkoris, E. Tsampasis, E. Klouvidaki, A.G. Boudouvis, V.N. Stathopoulos, Plug actuation and active manipulation in closed monolithic fluidics using backpressure, Microelectronic Engineering 216 (2019) 111046. https://doi.org/10.1016/j.mee.2019.111046.
[27] A. Kouloumpis, N. Vourdas, P. Zygouri, N. Chalmpes, G. Potsi, V. Kostas, K. Spyrou, V.N. Stathopoulos, D. Gournis, P. Rudolf, Controlled deposition of fullerene derivatives within a graphene template by means of a modified Langmuir-Schaefer method, Journal of Colloid and Interface Science 524 (2018) 388–398. https://doi.org/10.1016/j.jcis.2018.04.049.
[28] T. Kuznetsova, T. Kriger, Y. Chesalov, A. Boronin, A. Ishchenko, P.K. Pandis, V. Krivensov, G. Litvak, T. Larina, V. Sadykov, V.N. Stathopoulos, Specific structural features of LnZrOx (Ln: La, Sm) mixed oxides prepared by different methods, Progress in Natural Science: Materials International 28 (2018) 437–446. https://doi.org/10.1016/j.pnsc.2018.07.007.
[29] N. Vourdas, D.C. Moschou, K.A. Papadopoulos, D. Davazoglou, V.N. Stathopoulos, A new microfluidic pressure-controlled Field Effect Transistor (pFET) in digital fluidic switch operation mode, Microelectronic Engineering 190 (2018) 28–32. https://doi.org/10.1016/j.mee.2017.12.019.
[30] V.N. Stathopoulos, T. Kuznetsova, O. Lapina, D. Khabibulin, P.K. Pandis, T. Krieger, Y. Chesalov, R. Gulyalev, V. Krivensov, T. Larina, V. Sadykov, Evolution of bulk and surface structures in stoichiometric LaAlO3 mixed oxide prepared by using starch as template, Materials Chemistry and Physics 207 (2018) 423–434. https://doi.org/10.1016/j.matchemphys.2017.12.056.
[31] V. Chalkia, N. Tachos, P.K. Pandis, A. Giannakas, M.K. Koukou, M.Gr. Vrachopoulos, L. Coelho, A. Ladavos, V.N. Stathopoulos, Influence of organic phase change materials on the physical and mechanical properties of HDPE and PP polymers, RSC Adv. 8 (2018) 27438–27447. https://doi.org/10.1039/C8RA03839B.
[32] P. Chrysinas, G. Pashos, N. Vourdas, G. Kokkoris, V.N. Stathopoulos, A.G. Boudouvis, Computational investigation of actuation mechanisms of droplets on porous air-permeable substrates, Soft Matter 14 (2018) 6090–6101. https://doi.org/10.1039/C8SM00952J.
[33] V. Chalkia, E. Marathoniti, V.N. Stathopoulos, A facile method for the preparation of ceramic beads with hierarchical porosity, Ceramics International 43 (2017) 17238–17242. https://doi.org/10.1016/j.ceramint.2017.09.102.

[34] V. Sadykov, E. Sadovskaya, A. Bobin, T. Kharlamova, N. Uvarov, A. Ulikhin, Ch. Argirusis, G. Sourkouni, V. Stathopoulos, Temperature-programmed C18O2 SSITKA for powders of fast oxide-ion conductors: Estimation of oxygen self-diffusion coefficients, Solid State Ionics 271 (2015) 69–72. https://doi.org/10.1016/j.ssi.2014.11.004.
[35] A. Milionis, C. Noyes, E. Loth, I.S. Bayer, A.W. Lichtenberger, V.N. Stathopoulos, N. Vourdas, Water-Repellent Approaches for 3-D Printed Internal Passages, Materials and Manufacturing Processes 31 (2016) 1162–1170.
[36] A. Efstathiou, V. Stathopoulos, Lean Burn DeNOx ApplicationsStationary and Mobile Sources, in: 2015: pp. 587–610. https://doi.org/10.1002/9783527686605.ch26.
[37] O. Smorygo, A. Marukovich, V. Mikutski, V. Stathopoulos, S. Hryhoryeu, V. Sadykov, Tailoring properties of reticulated vitreous carbon foams with tunable density, Frontiers of Materials Science 10 (2016) 157–167. https://doi.org/10.1007/s11706-016-0338-8.
[38] N. Vourdas, G. Pashos, G. Kokkoris, A.G. Boudouvis, V.N. Stathopoulos, Droplet Mobility Manipulation on Porous Media Using Backpressure, Langmuir 32 (2016) 5250–5258. https://doi.org/10.1021/acs.langmuir.6b00900.
[39] G. Leontakianakos, I. Baziotis, V.N. Stathopoulos, Z. Kypritidou, L. Profitis, E. Chatzitheodoridis, S. Tsimas, Influence of natural water composition on reactivity of quicklime derived from Ca-rich and Mg-rich limestone: implications for sustainability of lime manufacturing through geochemical modeling, RSC Adv. 6 (2016) 65799–65807. https://doi.org/10.1039/C6RA11346J.
[40] P.K. Pandis, E. Xenogiannopoulou, P.M. Sakkas, G. Sourkouni, Ch. Argirusis, V.N. Stathopoulos, Compositional effect of Cr contamination susceptibility of La9.83Si6−x−yAlxFeyO26±δ apatite-type SOFC electrolytes in contact with CROFER 22 APU, RSC Adv. 6 (2016) 49429–49435. https://doi.org/10.1039/C6RA02025A.
[41] A.V. Yeganyan, A.S. Kuzanyan, V. Stathopoulos, Estimation of thermal conductivity coefficient for solid-state crystal dielectrics at high temperatures, Journal of Contemporary Physics (Armenian Academy of Sciences) 49 (2014) 176–179. https://doi.org/10.3103/S1068337214040070.
[42] G. Leontakianakos, I. Baziotis, A. Papandreou, D. Kanellopoulou, V.N. Stathopoulos, S. Tsimas, A comparative study of the physicochemical properties of Mg-rich and Ca-rich quicklimes and their effect on reactivity, Materials and Structures 48 (2015) 3735–3753. https://doi.org/10.1617/s11527-014-0436-y.
[43] V. Chalkia, P. Pandis, V. Stathopoulos, Shape Forming of Ceramic Tubes for Electrochemical Reactors by Gel-Casting Method, ECS Transactions 68 (2015) 2339. https://doi.org/10.1149/06801.2339ecst.
[44] N. Vourdas, K. Dalamagkidis, V.N. Stathopoulos, Active porous valves for plug actuation and plug flow manipulation in open channel fluidics, RSC Adv. 5 (2015) 104594–104600. https://doi.org/10.1039/C5RA21263D.
[45] N. Vourdas, C. Ranos, V.N. Stathopoulos, Reversible and dynamic transitions between sticky and slippery states on porous surfaces with ultra-low backpressure, RSC Adv. 5 (2015) 33666–33673. https://doi.org/10.1039/C5RA00663E.
[46] A. Zarkadoulas, V.N. Stathopoulos, Perovskites: Versatile Weaponry in the Arsenal of Energy Storage and Conversion, Energies 15 (2022). https://doi.org/10.3390/en15186555.
[47] O. Okogeri, V.N. Stathopoulos, What about greener phase change materials? A review on biobased phase change materials for thermal energy storage applications,

International Journal of Thermofluids 10 (2021) 100081. https://doi.org/10.1016/j.ijft.2021.100081.

[48] E. Douvi, C. Pagkalos, G. Dogkas, M.K. Koukou, V.N. Stathopoulos, Y. Caouris, M.Gr. Vrachopoulos, Phase change materials in solar domestic hot water systems: A review, International Journal of Thermofluids 10 (2021) 100075. https://doi.org/10.1016/j.ijft.2021.100075.

[49] G. Dogkas, J. Konstantaras, M.K. Koukou, M. Gr. Vrachopoulos, C. Pagkalos, V.N. Stathopoulos, P.K. Pandis, K. Lymperis, L. Coelho, A. Rebola, Development and experimental testing of a compact thermal energy storage tank using paraffin targeting domestic hot water production needs, Thermal Science and Engineering Progress 19 (2020) 100573. https://doi.org/10.1016/j.tsep.2020.100573.

[50] G. Dogkas, M.K. Koukou, J. Konstantaras, C. Pagkalos, K. Lymperis, V. Stathopoulos, L. Coelho, A. Rebola, M.Gr. Vrachopoulos, Investigating the performance of a thermal energy storage unit with paraffin as phase change material, targeting buildings' cooling needs: an experimental approach, International Journal of Thermofluids 3–4 (2020) 100027. https://doi.org/10.1016/j.ijft.2020.100027.

[51] M.K. Koukou, G. Dogkas, M.Gr. Vrachopoulos, J. Konstantaras, C. Pagkalos, V.N. Stathopoulos, P.K. Pandis, K. Lymperis, L. Coelho, A. Rebola, Experimental assessment of a full scale prototype thermal energy storage tank using paraffin for space heating application, International Journal of Thermofluids 1–2 (2020) 100003. https://doi.org/10.1016/j.ijft.2019.100003.

[52] M.K. Koukou, G. Dogkas, M.Gr. Vrachopoulos, J. Konstantaras, C. Pagkalos, K. Lymperis, V. Stathopoulos, G. Evangelakis, C. Prouskas, L. Coelho, A. Rebola, Performance Evaluation of a Small-Scale Latent Heat Thermal Energy Storage Unit for Heating Applications Based on a Nanocomposite Organic PCM, ChemEngineering 3 (2019). https://doi.org/10.3390/chemengineering3040088.

[53] C.N. Elias, V.N. Stathopoulos, A comprehensive review of recent advances in materials aspects of phase change materials in thermal energy storage, Energy Procedia 161 (2019) 385–394. https://doi.org/10.1016/j.egypro.2019.02.101.

[54] A. Tremouli, I. Karydogiannis, P.K. Pandis, K. Papadopoulou, C. Argirusis, V.N. Stathopoulos, G. Lyberatos, Bioelectricity production from fermentable household waste extract using a single chamber microbial fuel cell, Energy Procedia 161 (2019) 2–9. https://doi.org/10.1016/j.egypro.2019.02.051.

[55] M.K. Koukou, M.Gr. Vrachopoulos, N.S. Tachos, G. Dogkas, K. Lymperis, V. Stathopoulos, Experimental and computational investigation of a latent heat energy storage system with a staggered heat exchanger for various phase change materials, Thermal Science and Engineering Progress 7 (2018) 87–98. https://doi.org/10.1016/j.tsep.2018.05.004.

[56] P. Nanou, A. Zarkadoulas, P. Pandis, I. Tsilikas, I. Katis, D. Almpani, N. Orfanoudakis, N. Vourdas, V. Stathopoulos, Micromachining on Stainless Steel 304 for Improved Water Condensation Properties, Key Engineering Materials 962 (2023) 19–26. https://doi.org/10.4028/p-FwZKv7.

[57] P. Nanou, J. Konstantaras, A. Zarkadoulas, L. Montorsi, H. Jouhara, V. Stathopoulos, Development and Evaluation of Corrosion Resistance and Hydrophobic Properties of Thermal Sprayed Coatings over Carbon Steel, Key Engineering Materials 963 (2023) 27–36. https://doi.org/10.4028/p-sth09H.

[58] P.K. Pandis, S. Papaioannou, V. Siaperas, A. Terzopoulos, V.N. Stathopoulos, Evaluation of Zn- and Fe- rich organic coatings for corrosion protection and condensation performance on waste heat recovery surfaces, International Journal of Thermofluids 3–4 (2020) 100025. https://doi.org/10.1016/j.ijft.2020.100025.
[59] N. Vourdas, H. Jouhara, S.A. Tassou, V.N. Stathopoulos, Design criteria for coatings in next generation condensing economizers, Energy Procedia 161 (2019) 412–420. https://doi.org/10.1016/j.egypro.2019.02.095.
[60] V. Stathopoulos, V. Sadykov, S. Pavlova, Y. Bespalko, Y. Fedorova, L. Bobrova, A. Salanov, A. Ishchenko, V. Stoyanovsky, T. Larina, V. Ulianitsky, Z. Vinokurov, V. Kriventsov, Design of functionally graded multilayer thermal barrier coatings for gas turbine application, Surface and Coatings Technology 295 (2016) 20–28. https://doi.org/10.1016/j.surfcoat.2015.11.054.
[61] I. Iliopoulos, A. Karampekios, P.K. Pandis, N. Vourdas, H. Jouhara, S. Tassou, V.N. Stathopoulos, Evaluation of organic coatings for corrosion protection of condensing economizers, Procedia Structural Integrity 10 (2018) 295–302. https://doi.org/10.1016/j.prostr.2018.09.041.
[62] N. VOURDAS, E. MARATHONITI, P.K. PANDIS, Chr. ARGIRUSIS, G. SOURKOUNI, C. LEGROS, S. MIRZA, V.N. STATHOPOULOS, Evaluation of LaAlO3 as top coat material for thermal barrier coatings, Transactions of Nonferrous Metals Society of China 28 (2018) 1582–1592. https://doi.org/10.1016/S1003-6326(18)64800-9.
[63] C. Morgante, X. Ma, X. Chen, D. Wang, V. Boffa, V. Stathopoulos, J. Lopez, J.L. Cortina, A. Cipollina, A. Tamburini, G. Micale, Metal-Organic-Framework-based nanofiltration membranes for selective multi-cationic recovery from seawater and brines, Journal of Membrane Science 685 (2023) 121941. https://doi.org/10.1016/j.memsci.2023.121941.
[64] P. Nanou, J. Konstantaras, A. Zarkadoulas, P.K. Pandis, N. Vourdas, V.N. Stathopoulos, Construction, Evaluation, and Performance of a Water Condensation Test Unit, Advances in Science and Technology 133 (2023) 35–43.
[65] P. Pandis, E. Michopoulos, C. Arvanitis, C. Argirusis, V. Stathopoulos, G. Lyberatos, A. Tremouli, Bioenergy Production from Tannery Waste via a Single-Chamber Microbial Fuel Cell with Fly Ash Cathodic Electrodes, Key Engineering Materials 962 (2023) 105–112. https://doi.org/10.4028/p-0xWsyq.
[66] P. Pandis, M. Georgala, P. Nanou, V. Stathopoulos, Fabrication and Study of 3D Printed ABS-Carbon Composite Anodes for Single Chamber Microbial Fuel Cells, Key Engineering Materials 962 (2023) 113–120. https://doi.org/10.4028/p-3QcQuv.
[67] Aristofanis Vollas, Vassilis Stathopoulos, Paraskevi Oikonomou, Detection of post-fire soil contamination using inductively coupled plasma-mass spectrometry (ICP-MS) in wildfire affected areas in Greece, in: EMANATE 2023 CONFERENCE PROCEEDINGS, 2023: p. 6.
[68] Nikolaos Vourdas, Maria Aptoglou, Vassilios Stathopoulos, Implementation of green special processes in aerospace industry, in: EMANATE 2023 CONFERENCE PROCEEDINGS, 2023: p. 20.
[69] Pavlos K. Pandis, Vassilis Stathopoulos, Structural and catalytic properties of manganese-based mixed oxides, in: EMANATE 2023 CONFERENCE PROCEEDINGS, n.d.: p. 23.

[70] Athanasios Zarkadoulas, Vassilis Stathopoulos, Vasileios Kyriakou, Development of redox stable, bi-functional cathodes for reversible solid oxide cells, in: EMANATE 2023 CONFERENCE PROCEEDINGS, 2023: p. 13.
[71] Pavlos K. Pandis, Maria G. Savvidou, Diomi Mamma, Georgia Sourkouni, Nikolaos Argirusis, Vassilis N. Stathopoulos, Christos Argirusis, Bioenergy production from tannery waste via a single-chamber Microbial Fuel Cell with steel anodes and Escherichia coli (E. coli), in: EMANATE 2023 CONFERENCE PROCEEDINGS, 2023: p. 22.
[72] Paraskevi Nanou, Pavlos K. Pandis, Athanasios Zarkadoulas, Ioannis Konstantaras, Ioannis Tsilikas, Ilias Katis, Despoina Almpani, Vassilis Stathopoulos, Preparation of super-hydrophobic surface: Study on the Effects of Sandblasting stainless steel, in: EMANATE 2023 CONFERENCE PROCEEDINGS, 2023: p. 25.
[73] Paraskevi Nanou, Athanasios Zarkadoulas, Vassilis Stathopoulos, Durable bi-functional coating on stainless steel 304, in: EMANATE 2023 CONFERENCE PROCEEDINGS, 2023: p. 17.
[74] Paraskevi Nanou, Athanasios Zarkadoulas, Oana Doina Trusca, Vassilis Stathopoulos, Development and evaluation of thermal sprayed corrosion protective coatings over engineering alloys, in: EMANATE 2023 CONFERENCE PROCEEDINGS, 2023: p. 15.
[75] Athanasios Zarkadoulas, John Konstantaras, Vassilis Stathopoulos, Maria Koukou, Michail Vrachopoulos, Functional coatings for smooth operation and stable performance of flat-type solar panels under various conditions, in: EMANATE 2023 CONFERENCE PROCEEDINGS, 2023: p. 12.